

Delft University of Technology  
Master of Science Thesis in Embedded Systems

# Integrated Communication and Sensing with RGB LEDs

Yixun Yan





# Integrated Communication and Sensing with RGB LEDs

Master of Science Thesis in Embedded Systems

Embedded and Networked Systems Group  
Faculty of Electrical Engineering, Mathematics and Computer Science  
Delft University of Technology  
Van Mourik Broekmanweg 6, 2628 XE Delft, The Netherlands

Yixun Yan

11/22/2021

**Author**

Yixun Yan

**Title**

Integrated Communication and Sensing with RGB LEDs

**MSc Presentation Date**

11/29/2021

**Graduation Committee**

Prof. Fernando Kuipers    Delft University of Technology

Dr. Qing Wang            Delft University of Technology

Dr. Jie Yang                Delft University of Technology

## Abstract

Visible Light Communication (VLC) has gained popularity due to its inherent security as a complementary technology to Radio Frequency (RF) in the last decades to solve the “spectrum crunch” problem. Meanwhile, The latest IEEE 802.11ah standard, also called WiFi HaLow, offers the range, throughput, and low power consumption that is extremely suitable for most simple IoT appliances for industrial, agricultural, and smart city environments. In general, these IoT products are connected in huge numbers. Hence, provisioning these simple IoT products that usually do not have any user interface like a keyboard or a display in a simple, robust, secure, and scalable method is a significant challenge.

VLC technology has been intriguing both industry and academia for connecting IoT products over the last few years. The signals used in VLC, the visible light, can be captured by eyes and be confined by walls and other blockages which introduce the security against eavesdropping. Besides, the features of low deployment cost, high throughput and high security make VLC a solution to provision IoT products securely. This project exploits on-device existing RGB LEDs to achieve a low-cost and secure device provision system called Integrated Visible Light Communication and Sensing (I-VLCS) System with the functionality of the integrated communication and sensing with RGB LEDs. Visible Light Positioning (VLP), a subset of Visible Light Sensing, is also used in the I-VLCS system to further improve the system security. The performance of the proposed I-VLCS system is evaluated through experiments, demonstrating that that the system can support a maximum 50 cm of communication range with a high communication and positioning accuracy.



# Preface

This report is the consolidation of my Master of Science thesis with the Embedded and Networked Systems (ENS) group over a period of ten months.

This thesis is submitted for the degree of Master of Science at the Delft University of Technology. It has been ten months since I started this project and the end is approaching now. I would like to express my thanks to every one who has been instrumental through the completion of this project.

Foremost, I would like to express my gratitude to my daily supervisor, Dr. Qing Wang for his patient guidance, selfless support and immense knowledge throughout my thesis. Due to the COVID-19 since last year, the communication is through online video meetings, making the completion of my thesis harder. Dr. Qing Wang introduced me into this fascinating VLC project and keeps providing me with constructive insights and solid feedback in the research problems, thesis work and presentation slides. This project could not be finished without his generous support. I also want to thank Hao Liu, another master's student in TU Delft who helped me draw the PCB board of the system. Special thanks go to Prof. Fernando Kuipers and Dr. Jie Yang for being the chair and the committee member of my thesis defense, respectively. Lastly, I would like to thank my parents for being the pillar of strength and support during this period and to all my friends in the Netherlands. Their loves are the motivation of the successful completion of my thesis.

Yixun Yan

Delft, The Netherlands  
22nd November 2021



# Contents

<b>Preface</b>	<b>v</b>
<b>1 Introduction</b>	<b>1</b>
1.1 Problem Statement . . . . .	2
1.2 Contributions . . . . .	4
1.3 Organization . . . . .	4
<b>2 Background and Related Work</b>	<b>5</b>
2.1 Visible Light Communication . . . . .	5
2.1.1 LEDs as transceivers . . . . .	5
2.1.2 RGB LEDs as transceivers . . . . .	8
2.2 Visible Light Positioning . . . . .	9
2.2.1 Received signal strength . . . . .	9
2.2.2 Angle of arrival . . . . .	11
2.2.3 Time and time difference of arrival . . . . .	11
<b>3 System Design</b>	<b>13</b>
3.1 System Overview . . . . .	13
3.2 Communication Protocol . . . . .	15
3.2.1 Frame format . . . . .	15
3.2.2 Communication process . . . . .	16
3.3 Characteristics of Tx and Rx . . . . .	18
3.3.1 Effects of lens and forward current . . . . .	18
3.3.2 Effects of distance and light intensity . . . . .	19
3.4 Responsivity . . . . .	20
3.5 Coding Scheme . . . . .	22
3.5.1 Encoding . . . . .	22
3.5.2 Decoding . . . . .	23
3.6 Color Selection . . . . .	24
3.7 Positioning Method . . . . .	25
<b>4 Implementation</b>	<b>29</b>
4.1 Overview . . . . .	29
4.2 Hardware Implementation . . . . .	30
4.2.1 Transmitter . . . . .	30
4.2.2 Receiver . . . . .	33
4.3 Software Implementation . . . . .	34
4.4 Finite-state machine (FSM) . . . . .	36

4.4.1	FSM of Tx and Rx . . . . .	36
4.4.2	FSM of serial communication . . . . .	36
4.4.3	User interface . . . . .	37
<b>5</b>	<b>Performance Evaluation</b>	<b>39</b>
5.1	Experimental Setup . . . . .	39
5.2	Noise Measurement . . . . .	40
5.3	Communication Performance . . . . .	41
5.4	Positioning Performance . . . . .	44
<b>6</b>	<b>Conclusions and Future Work</b>	<b>47</b>

## Terms and abbreviations

<b>Terms</b>	<b>Description</b>
ACK	Acknowledgement segment
ADC	Analog-to-Digital Converter
AOA	Angle Of Arrival
APP	Applications on Smartphones
BER	Bit Error Ratio
CRC	Cyclic Redundancy Check
FOV	Field Of View
FSM	Finite State Machine
IoT	Internet of Things
IPS	Indoor Positioning System
IR	Infrared Radiation
I-VLCS	Integrated Visible Light Communication and Sensing
k-NN	k-Nearest Neighbors algorithm
LED	Light-Emitting Diode
LOS	Light-Of-Sight
MAC	Medium Access Control
MCU	Micro-controller
MLAT	Multilateration
NFC	Near Field Communication
RF	Radio Frequency
RFID	Radio Frequency Identification
RGB	Red-Green-Blue
RSS	Received Signal Strength
Rx	Receiver
SSID	Service Set Identifier
TDOA	Time Difference Of Arrival
TIA	Trans-Impedance Amplifier
TOA	Time Of Arrival
Tx	Transmitter
USB	Universal Serial Bus
VLC	Visible Light Communication
VLS	Visible Light Sensing
VLP	Visible Light Positioning
WDM	Wavelength Division Multiplexing



# Chapter 1

## Introduction

With the increasing pressure from “spectrum crunch” on the Radio Frequency (RF) spectrum in recent years, Visible Light Communication (VLC) is gaining popularity as an emerging alternative to conventional RF communication. Visible light can be captured by eyes and can be easily confined by walls or other obstacles, we can also control the communication through the directivity and the visual field of light propagation which makes the VLC much more secure against eavesdropping compared with traditional RF communication. A typical VLC system usually consists of two components: a transmitter and a receiver. The transmitter normally modulates and transmits data by emitting visible lights from 380 nm to 780 nm wavelength by a light source through the Light-of-Sight (LOS) channel to the receiver. The receiver uses a photo-detector which can be a photodiode, a camera or an image sensor, or a LED to demodulate and decode the incident lights based on received optical power on the receiver surface.

So far, many application scenarios have been exploited with the VLC system. For example, LEDs can be used as receivers just like photodiodes to measure the incident light in point-to-point links which are referred to as LED-to-LED communication [6, 13, 27]. Lots of Indoor Positioning Systems (IPS) also use LEDs emerged in recent years which leverage the VLC techniques and achieved even better accuracy compared to some RF-based IPS [47]. In addition, there are many other VLC application scenarios developed such as high-speed communication [14, 40], vehicle-to-vehicle communication [41, 44, 45] and so on.

Today, it is common to have tens or even hundreds of devices connected to the internet in one household according to the increasing requirements of the Internet of Things (IoT). The wireless networking protocol IEEE 802.11ah, also called Wi-Fi HaLow was published [4] in 2017 which is specially designed for IoT networks as shown in Figure 1.1. Compared with conventional Wi-Fi networks (802.11 a/b/g/n) operating at either 2.4 GHz or 5 GHz, the Wi-Fi HaLow operating range spans 1 MHz to 16 MHz channels with a sub-1 GHz spectrum which brings wider coverage range (1 km outdoor) and higher data rates (80 Mbps can be reached using 16 MHz channel) [2]. It also benefits from supporting up to 8191 devices per access point and lower energy consumption which allows a large number of devices or sensors that cooperate to share signals. All the advantages above make Wi-Fi HaLow one of the most suitable protocols for connecting IoT devices.

Wi-Fi provisioning is the process of connecting a new Wi-Fi device or a station

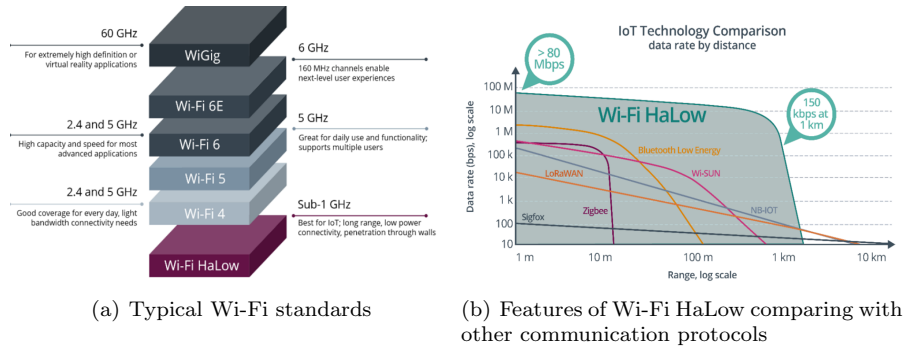


Figure 1.1: **General information of Wi-Fi HaLow** [2, 3]

to a Wi-Fi network, which involves loading the station with the network name (usually referred to as SSID) and its security credentials (usually referred to as password). While the provisioning of a large amount of IoT devices in a secure and scalable method is a significant challenge and VLC is a possible solution as a complementary technology to RF due to its low power consumption and inherent security against eavesdropping. However, many IoT devices nowadays do not equip with a display and a keyboard or even a user interface at all which makes the users can not input data at each device directly, these devices need an alternative provisioning method that has to be simple to use and secure. Some existing provisioning techniques such as SmartConfig which leverages an APP in a smartphone to provision the network or some out-of-band methods such as using Bluetooth/NFC/USB to connect an extended user interface are not secure, not scalable, or add a lot of extra costs. Meanwhile, almost all IoT devices have existing RGB LEDs used for indication or debugging, which means there is no other extra sensor is required. All these advantages make LED-to-LED communication a possible solution to provisioning massive Wi-Fi HaLow IoT devices securely in a scalable way without extra costs.

## 1.1 Problem Statement

The objective of this thesis is to exploit on-device existing RGB LEDs to achieve a low-cost and secure device provision system for provisioning massive Wi-Fi HaLow IoT devices, where the enabler is the integrated communication and sensing with RGB LEDs. The advantage of LED-to-LED communication in VLC and Visible Light Positioning (VLP) will be integrated to communicate and sense simultaneously in our system. However, most published LED-to-LED communication systems only concentrate on characterizing the single color LEDs as photo-detectors. These systems usually need large and expensive single-color LEDs and extra sensors such as image sensors. While we noticed that almost all IoT devices have RGB LEDs for indicating or debugging, these RGB LEDs can be used as both transmitters and receivers in a VLC system. There are only a few pieces of research on deploying RGB LEDs instead of single-color LEDs in LED-to-LED communication and only a few experiments on the characteristics of an off-the-shelf cheap RGB LED [11, 12] have been done which introduce

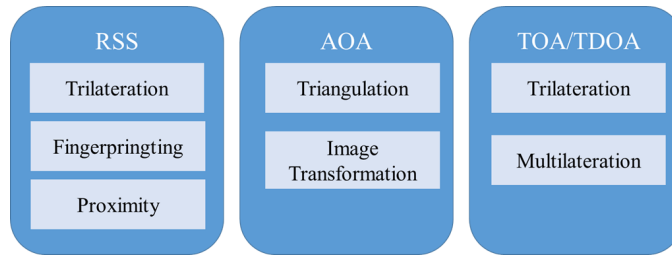


Figure 1.2: **Category of LED positioning algorithms**

the significant difficulty in the implementation of the communication part with RGB LEDs in the I-VLCS system.

Another challenge that exists in the I-VLCS system is the implementation of the VLP technique in sensing and positioning functionality. There are three typical categories of positioning models divided by received optical signals: Received Signal Strength (RSS), Angle of Arrival (AOA), and Time of Arrival (TOA) or Time Difference of Arrival (TDOA) [8, 47, 18], respectively. The taxonomy of mainstream positioning algorithms for each model is present in Figure 1.2. However, all these popular positioning algorithms have difficulty in the implementation in our system that uses only one off-the-shelf RGB LED simulating the RGB LEDs existing on most simple IoT devices without adding any extra sensors. For example, positioning methods based on conventional Trilateration and Triangulation algorithms should use multiple LEDs with known locations or only work in the pre-defined confined space. Both of them use geometric properties of triangles for location estimation but the distribution of LEDs on IoT devices are usually located parallelly or in a line which makes it is hard to implement these two algorithms. The fingerprinting method needs to collect the RSS values at each observed location in the off-line stage to store in the database, this training stage is too labor-intensive to implement in a simple IoT appliance. The rest popular algorithms such as Multilateration and Image Transformation ask the extra high-accuracy sensors for the IPS which is against the design of our system.

To achieve our objective to implement the I-VLCS system that leverages the advantages of VLC and VLP to provision massive IoT devices in a secure, scalable way without any extra sensors, the requirements are listed following:

1. The communication part of the system based on the VLC using RGB LEDs should be implemented, which is composed of uplink communication and downlink communication. The uplink communication is transmitting data messages from the receiver (Rx, representing IoT devices) to the transmitter (Tx, representing user devices such as smartphones or access points); and the downlink is the verse case.
2. Due to the difficulty in the implementation of the mainstream positioning algorithm mentioned above, a positioning method that only requires a pair of RGB LEDs (one at the Rx and one at the Tx) is proposed for the I-VLCS system. The sensing part, also called positioning of the system, should achieve a good performance using the proposed algorithm under the RSS-based model.

3. The performance of the I-VLCS system should be evaluated for essential parameters such as data rate, communication range, communication accuracy, positioning accuracy, etc. The effects of possible noises should be analyzed for improving the system performance.

## 1.2 Contributions

This thesis proposes I-VLCS, a system that leverages VLC and VLP to support provisioning IoT devices using existing RGB LEDs in a scalable, secure method. The mechanism designed in the system can solve the research problem presented in Section 1.1. The contributions of the thesis are summarized as follows:

1. Front-end optical transceivers are implemented using off-the-shelf RGB LEDs in the I-VLC system. The proposed modulation scheme, positioning algorithms, and tasks with great computation such as color recognition are implemented in the built-in MCU (AT91SAM3X8E) of Arduino Due [1].
2. A novel positioning algorithm is proposed for the I-VLCS system. The new positioning algorithm is based on the received signal strength and different responsivity of the photo-detector to different incoming light angles, which only uses one RGB LED in transceivers and achieves good accuracy in positioning and communicating simultaneously.
3. The performance of the I-VLCS system is evaluated for both the communication and sensing parts. The k-Nearest Neighbors (k-NN) algorithm is used for color recognition at the Rx and the  $K$  value is determined based on the experiment results. The communication accuracy of the current I-VLCS system can achieve higher 99.99% at designed communication distance in color\_4 Mode ModeType with 5 kHz transmitting frequency meanwhile the positioning accuracy of the current I-VLCS system achieves a maximum value of 99.8 % in the tested location at 10 cm and  $90^\circ$  estimated by the formulas calibrated at 10 cm distance.

## 1.3 Organization

The rest of the thesis is organized as follows: Chapter 2 provides the background knowledge on VLC, VLP and provides an overview of the related work. The system design of I-VLCS, including the communication protocol, color selection, coding scheme and positioning method, is presented in Chapter 3. Details of the implementation of the transceiver in the I-VLCS system are presented in Chapter 4, followed by the experimental evaluation of the system in Chapter 5. Finally, The conclusion of the thesis along with the future work are summarized in Chapter 6.

## Chapter 2

# Background and Related Work

This chapter first presents some background information and related work on VLC using LED or RGB LED as transceivers in Section 2.1. Then the state-of-the-art VLP methods are discussed in Section 2.2.

### 2.1 Visible Light Communication

As a complementary technology to RF, VLC has gained popularity due to its low power consumption and inherent security against eavesdropping in the last few decades to solve the wireless "spectrum crunch" caused by the formidable uptake of cellular communication and connected devices in the era of IoT [17]. The signals transmitted in VLC, the visible lights ranging from 430 THz to 770 THz, can not penetrate the obstacles like walls which results in the safety against hacking by outside not in LOS channel with the transmitter. The previous research in VLC can be divided into two directions: i) The first direction is improving the bandwidth, range and throughput of the VLC to complement and compete with RF communication technologies, which can be deployed on the high-speed network and telephony technologies but too expensive and complicated to implemented on simple IoT devices. ii) The other direction considers applying VLC in simple IoT devices that require low cost, wide availability and easy commercial deployments and these applications usually require only infrequent communication with relatively low data speed and throughput over a short communication range which is the direction followed by the the I-VLCS system proposed in our project. Following this low-cost direction, LEDs are the transceivers selected in the designed system, which are the core of contemporary energy-efficient lighting and are widely implemented in commercial smart devices, while they can also be deployed as VLC transceivers and this technique is called LED-to-LED communication.

#### 2.1.1 LEDs as transceivers

Figure 2.1 presents a general architecture of a typical VLC system, in which only shows the single-direction link from the transmitter to the receiver (downlink

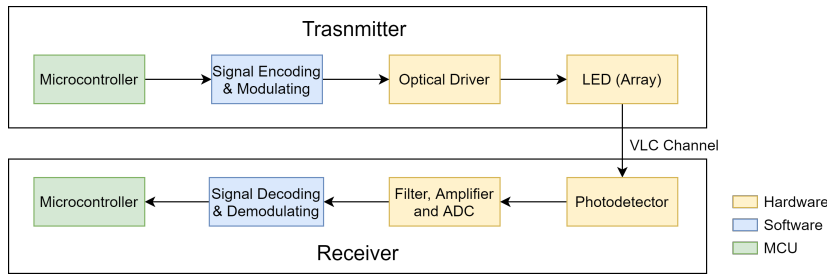


Figure 2.1: **General architecture for a VLC system**

communication). Both receiver and transmitter devices include the hardware and software parts. The infrastructure of the transmitter has the optical driver and the micro-controller to handle the modulation and encoding of the data. The data should be transmitted through the VLC optical channel. The received signal will be amplified and filtered before demodulation and the final position is usually presented to the user interface after decoding. Usually, the photodetector of the receiver in a typical VLC system is selected from the following three types of photo-sensors. In a VLC system, the photo-sensor of the receiver usually choose from the following three types of photo-sensors:

1. *Photodiode*: Photodiode (PD) is a semiconductor device that can generate photo-current based on the optical power of incident lights received at the photo-sensitive surface, the off-the-shelf PDs in market can achieve the sample rate at of tens of MHz.
2. *Cameras*: Cameras are widely deployed in VLC systems to receive modulated lights by its rolling shutter effect. These high-accuracy sensors usually bring a higher communication accuracy and a wider range while introducing the extra costs as well. However, VLC systems based on cameras can not support high data rates due to the limitation of the camera's sampling rate during communication.
3. *LED*: LEDs can sense the lights if it is operated in a reverse-biased voltage. It is normally a less sensitive and narrow field of view compared with PDs, but the low power consumption, the ubiquitous implementation, and the low cost make LEDs appealing to act as a photo-detector in a VLC system that communicates infrequently at a low data rate and a short communication range.

Due to the target devices being simple IoT devices and only needing to transmit data infrequently for provisioning the network in our thesis, the LED is selected as the photo-detector used in the designed system. As present in Figure 2.2(a), the LED works as a p-n junction diode that emits lights when activated under the forward biased condition, which is its common use in most applications as a power-on or debugging indicator. While the LED can function as a PD giving the reverse-biased condition in Figure 2.2(b) to sense incident light based on the photo-electric effects following the equation:

$$I_p = \int_{\lambda} S(\lambda) \cdot \eta(\lambda) \cdot A_{PD} d\lambda , \quad (2.1)$$

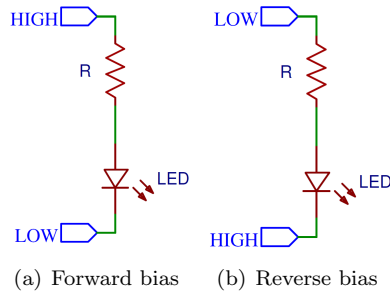


Figure 2.2: **Emitting and sensing light with a LED**

where  $S(\lambda)$  is the spectral irradiance ( $W/m^{-2}\cdot nm^{-1}$ ) impinging on the LED,  $\eta(\lambda)$  is the responsivity ( $A/W$ ) and  $A_{PD}$  is the photo-sensitive area of the PD/LED.

As an appealing approach, VLC using LEDs have many key features that are suitable for small networked IoT devices: Firstly, LEDs are widely used in all residential and commercial indoor environments which are "green" technology with quite low energy consumption (100 mW for 10-100 Mbps) [16, 47]. And LED-to-LED communication provides a method for IoT devices to communicate with each other over the free-space optical line-of-sight channel and typically achieve a throughput of less than one megabit per second at a distance of no more than a few meters [36, 34]. In addition, the adoption of VLC does not have health hazards caused by the electromagnetic generated by RF. Another advantage of LEDs is cost-efficient and a long lifetime (up to 10 years with reliable illumination) while having a cheap fee [37, 31]. These features make LED-to-LED VLC networks useful when deploying scenarios that need to add or remove endpoints frequently or cost sensitivity such as deploying smart home networks, sensor networks, or consumer devices like smart toys. These IoT devices do not require transmitting data frequently at a high data rate and their LEDs are usually used for data reception and can leverage the ubiquitous presence of LEDs such as the residential and office where white LEDs are widely used as lighting devices to configure the LED-to-LED communication network. Besides, the communication using LEDs has negligible effects on the level of brightness of LEDs so there is little effect on its illumination work. Last but not most important, VLC using LEDs is more secure than wireless RF communication which prevents eavesdroppers from hacking the networks [7] because the visible light cannot penetrate walls or other opaque obstructions which also makes it do not interfere with each other in different rooms [21].

There are lots of relevant research that has been done in the VLC system using LEDs. In the direction of deploying LEDs in simple devices, Miyazaki's work [28] firstly proposed using LEDs as a wavelength-selective photo-detector for ambient light. Then Dietz' et. al work [6] designed a system that uses a single LED as both a light source and a sensor to make an LED as a wireless serial data port to transmit and receive data. Later, researchers at Disney research labs [13, 36, 5, 35] proposed LED-to-LED communication systems that focus on the storing energy ability of LEDs to decrease the energy consumption of small commercial devices like toys. Their works are based on the charging and discharging of capacitors and can only achieve very low data rates. On the

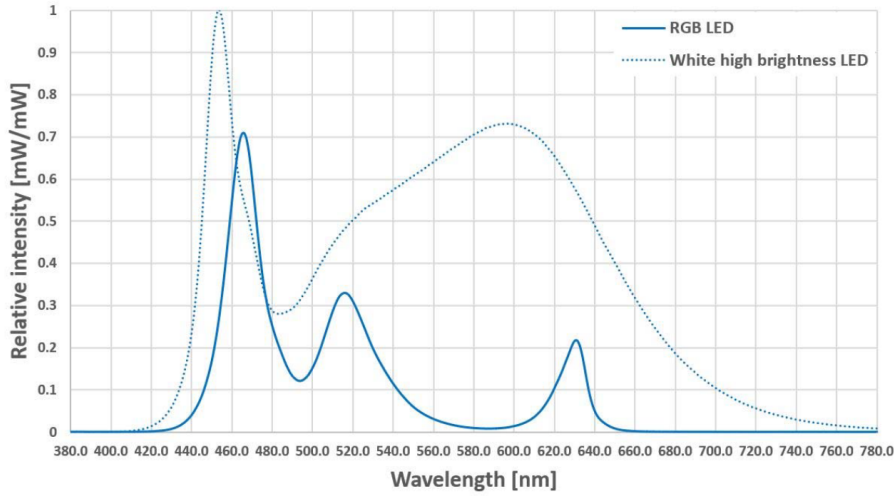


Figure 2.3: **Spectrum of an RGB LED and a blue-phosphorus LED [12]**

other hand, the works [22, 38] concentrate on exploiting the potential of LEDs working as transceivers to increase the data rate of the LED-to-LED channels were published. These works also employed the Trans-Impedance Amplifier (TIA) circuit in the systems which are also deployed in our system. Besides, Kowalczyk et. al [32, 26] studied the best wavelength of each single-color LED and proved the LED as a photo-detector having much higher bandwidth than its modulation bandwidth and their further work focusing on increasing improves the bandwidth of LED photo-detectors to maximize the performance of the LED as a photo-detector and optimize the design of the transmitter and receiver circuit of the LED-to-LED communication system.

### 2.1.2 RGB LEDs as transceivers

The research mentioned in previous Section 2.1.1 aiming at characterizing single-color LEDs as photo-detectors, but did not consider implementing off-the-shelf Red-Green-Blue (RGB) LEDs instead which are usually existing on most commercial IoT products for indication or debugging. RGB LEDs are composed of 3 sub-LEDs that emit red, green, and blue light respectively which usually have a common terminal (anode or cathode). Some research [24, 10] has been done to exploit the characteristics of using RGB LEDs as photo-detectors in VLC system and exploit the combination of transmitter and detect sub-LEDs of an RGB LED and test the angular characteristics of RGB LEDs as photo-detectors. As shown in Figure 2.3 which presents the spectrum of an RGB LED and blue phosphorus LED [10], there are 3 peaks of RGB LEDs' spectrum referring to three sub-LEDs emitting red, green and blue lights respectively. The RGB LED receiver can separate the color of incoming light signal on their sub-LEDs separately according to the different responsivity due to the variety in wavelength of each color of incident lights. Compared to characterizing single-color LEDs as photo-detectors, RGB LEDs should achieve higher data rates in the same VLC system.

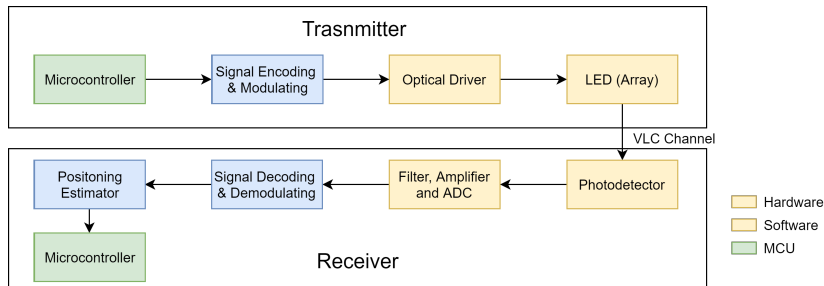


Figure 2.4: **General architecture for a simplex VLP system**

Although the previous work mentioned tested the characteristics of RGB LEDs as photo-detectors, the experimental results are quite different depending on the selection of LEDs. Hence, the characteristics of RGB LEDs implemented in our system as both transmitter and receiver are tested in Section 3.4 which is the fundamental of the "color selection" for communication and positioning in the I-VLCS system.

## 2.2 Visible Light Positioning

As introduced in Section 1.1, three mainstream categories of positioning methods are RSS, AOA, and TOA/TDOA based on the characteristics of signal strength, angular characteristics, and time of arrival at the receiver side respectively. A general architecture for a simplex VLC positioning system is shown in Figure 2.4. Typically, the positioning process at the receiver side consists of two steps: First of all, the processor demodulates and decodes the frame transmitting via the VLC channel which should consist of any LOS paths from the transmitter to the receiver. Then the receiver can estimate its location based on the chosen positioning algorithms.

### 2.2.1 Received signal strength

The RSS method is the most commonly implemented methods in IPS because it is usually easy to implement which only need a photo-detector to receive the values representing signal strength without extra auxiliary devices. It is also the positioning model deployed in the I-VLCS system. The most classical algorithms based on RSS model are *Trilateration*, *Fingerprinting* and *Proximity*, while all of them are not suitable in our system due to their limitations. The introduction of these three positioning algorithms and their limitations are listed as follows:

1. *Trilateration*: The positioning system based on trilateration algorithms [19, 23, 15, 43] needs at least three LEDs with known locations which are usually distributed in three different directions of the receiver as shown in Figure 2.5(a). However, the distribution of RGB LEDs on most IoT devices are in a line or parallel. The photo-detector deployed in our system, the three sub-LEDs packaged in an RGB LED, can be seen as located at one point in space. Obviously, the simple implementation of conven-

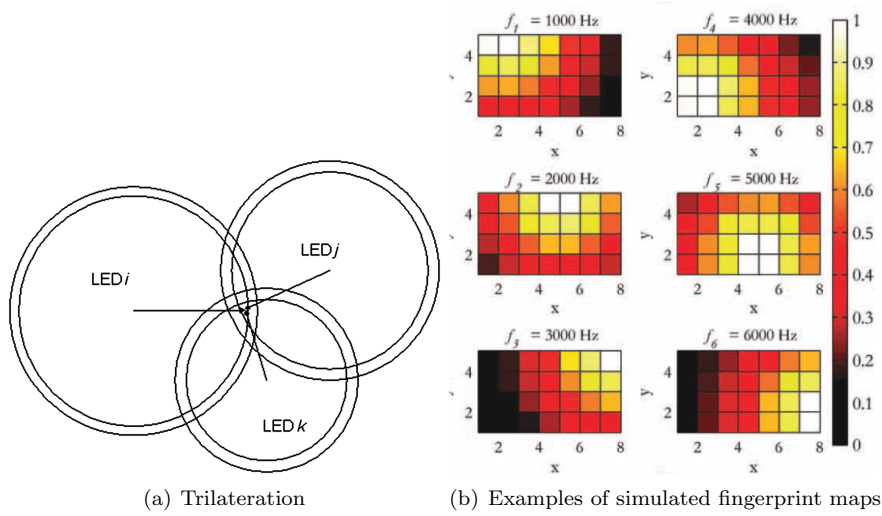


Figure 2.5: **Trilateration and examples of fingerprint maps [39, 15]**

tional trilateration in our system will lead to a bad performance in positioning accuracy due to the distribution of sub-LEDs.

2. *Fingerprinting*: Fingerprinting method [29] is widely used in RF-based IPS, which mainly consists of two steps: the offline survey and the online positioning. Fingerprinting divided a known space into multiple grids and each of them is a testing location. At the offline survey stage, the receiver collects the sensed value at every test grid and records the data in the database. At the online positioning stage, the receiver compares the sensed values generated by the optical signals from the target device with the database to estimate the relative location of the target. However, the offline stage is quite labor-intensive in fingerprinting to collect the data in every pre-defined grids and this method is confined in a specific area that is not suitable for provisioning massive devices. Figure 2.5(b) presents a result using fingerprinting, a specific space is divided into multiple fingerprint locations which have the corresponding data collected in the offline stage in the database. The choice of grid size is important which directly influences the positioning accuracy meanwhile it adds extra work in the offline training process.
  
3. *Proximity*: So far, proximity algorithms have been mainly employed in Infrared Radiation (IR), RFID and Bluetooth [25, 46, 9] which can roughly estimate the relative location information by comparing the strongest signals with the previously known locations of transmitters. It is easy to implement but not very accurate because of the requirements of a high density of transmitter distribution.

### 2.2.2 Angle of arrival

AOA-based positioning model uses the difference in responsiveness of receivers of the angle between the light of the sight and the normal angle of incident light. Compared to the RSS method, AOA usually can achieve very good positioning accuracy, but its algorithms such as triangulation models and image transformation require deploying expensive extra sensors like an array of image sensors at the receiver side to locate the target instead of positioning directly. Hence, it adds the budget for auxiliary sensors.

1. *Triangulation:* Triangulation is still the most widely used algorithm to position among AOA-based IPS. There are two types of methods using triangulation under AOA based model: trilateration and angulation. Both of them deploy the geometric properties of triangles to estimate the location of the target. The difference is that the former method which is called lateration as well measures the distances to estimate the receiver location while the angulation method is based on measuring the difference of incoming angles at the receiver side.
2. *Image Transformation:* The image transformation method needs to take a photo and estimate the location based on the trigonometric relationship between transmitters and the receivers. This approach needs a high-accuracy camera because the resolution of the image and the FOV of the camera have a significant impact on positioning accuracy.

### 2.2.3 Time and time difference of arrival

TOA and TDOA require only simple photo-detectors such as photodiodes which is inexpensive but still needs multiple photo-detectors and very accurate time synchronization between transmitter and receiver.

1. *Trilateration:* Trilateration is also employed in TOA/TDOA methods based on the time difference of the light traveling a certain communication distance.
2. *Multilateration:* Multilateration (MLAT) which is also called hyperbolic navigation is another method used in TOA/TDOA-based system. It estimates the target locations by measuring the massive number of locations to multiple generate hyperbolic curves in the Cartesian coordinate to determine the target location.

The proposed I-VLCS system in this thesis aims to implement a system for provisioning small IoT devices that can communicate and sense the locations of target devices based on the VLC technique by using only existing RGB LEDs without extra sensors. Among the VLP algorithms introduced previously, the AOA-based system usually requires expensive sensors and TOA/TDOA requires known locations of receivers and very accurate time synchronization. Finally, the RSS-based model is adopted in our system but all three popular algorithms based on the RSS model do not meet our requirements. Hence, a new estimation algorithm based on the RSS model is proposed and deployed in the I-VLCS system for sensing and positioning target devices using only one RGB LED which will be introduced in Chapter 4 later.



## Chapter 3

# System Design

This chapter mainly presents the details of the proposed system in our project, i.e., the I-VLCS (Integrated Visible Light Communication and Sensing) system, which communicates and senses based on VLC technique using one RGB LED.

### 3.1 System Overview

The system architecture of the I-VLCS system is presented in Figure 3.1. As with other typical VLC systems, a complete I-VLCS system is composed of two types of devices: transmitters and receivers. Each device is composed of the hardware part and the software part, which communicates with each other via LOS optical channel or with the PC through USB. Recalling the research goals of the project, the transmitter and receiver both have a specific role to play in the system.

To communicate and sense the target devices in the I-VLCS system, there are mainly three steps. Firstly, a communication channel needs to be established using a two-way handshake method. Next, the transmitter sends frames with fixed color sequences in the payload segment to receivers for calibration. In this step, the receiver samples multiple times for each defined ColorType in the payload segment of the calibration frame and store their values in the database for the color recognition in decoding work when communicating. The devices can communicate and sense with each other after the calibration is finished, and re-calibration should be performed when the communication accuracy is lower than the pre-defined threshold value or the position of any device is moved.

From Figure 3.1, we can see that the transmitter and receiver have the same architecture in our system, which means that all devices can easily change their software-defined mode between transmitter (Tx) mode and receiver (Rx) mode.

In the Tx mode, the transmitter device works as follows:

1. Firstly, the device receives the data sent waiting for encoding and modulating generated by the PC terminal such as the SSID or password for provisioning. This process is done by PC terminals in our system.
2. The data is then encoded into a color sequence of lights. Every chosen color represents a specific bit sequence that is pre-defined by the ModeType segment of the frame together with the coding scheme in the protocol.

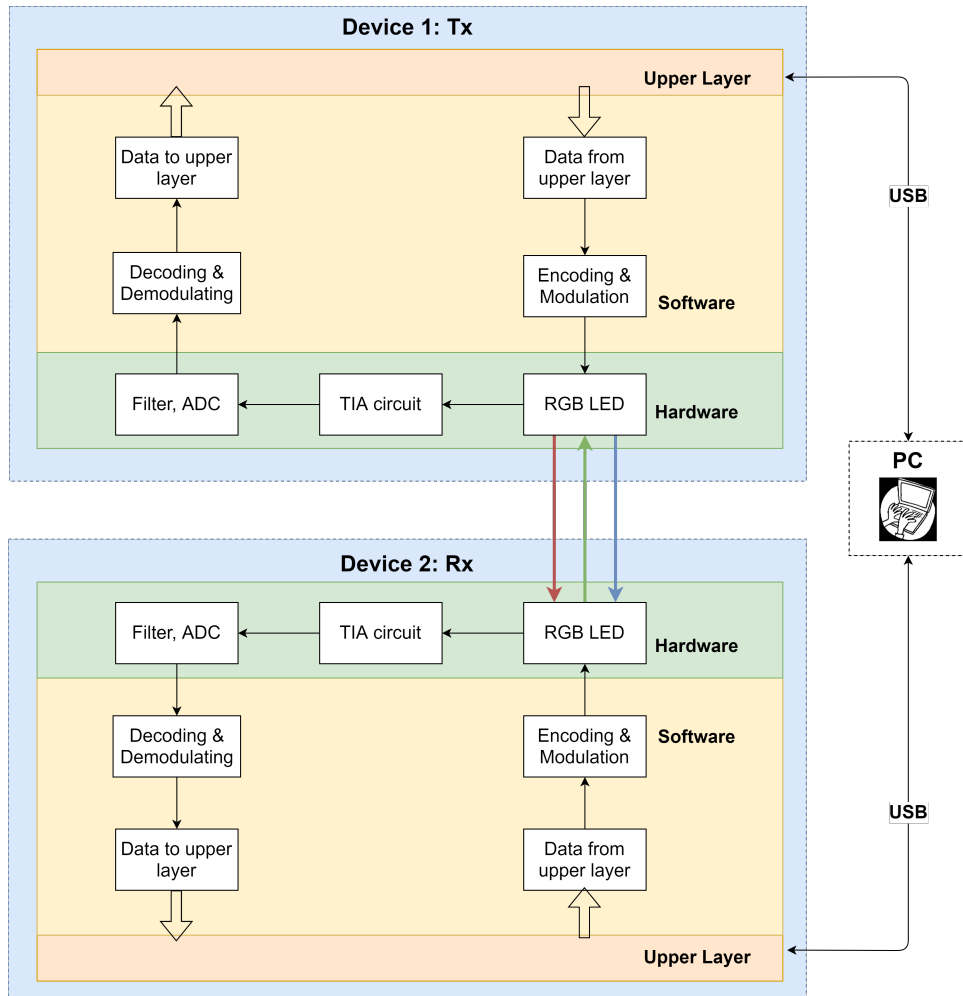


Figure 3.1: The system architecture of the proposed I-VLCS (Integrated Visible Light Communication and Sensing) system

3. The RGB LED is forward-biased to emit the color sequences of the light. It waits for incoming signals or keeps sending data depending on the device's current state.

An the Rx side, the RGB LED is reverse-biased as a photo-detector and work as follows:

1. The incoming lights received by the reverse-biased RGB LEDs will generate a sequence of photo-currents due to the different responsivity of sub-LEDs to lights with different wavelengths.
2. The current will be converted into voltages and get amplified through the TIA circuit.
3. The amplified voltages will be filtered and converted into digital values by the ADC. The MCU will perform the color recognition by comparing

the sensed values at pins and the data of each ColorType stored in the database measured in the calibration stage.

4. The data will be sent to the PC terminal and stored in files via USB for further work such as debugging, evaluation, or generating fitting curves for positioning.

The main properties of the I-VLCS system are introduced in detail in the rest of this chapter as follows:

- A communication protocol and the frame format are designed to enable the VLC and positioning in Section 3.2.
- The effects of lens and characteristics of the system including the effects of distance, light intensity, and forward current through the transmitter are presented in Section 3.3.1 and Section 3.3.2.
- The responsivity of all Tx - Rx combinations and the angular characteristic of the selected LED's responsivity is present in Section 3.4.
- The design of the coding scheme is presented in Section 3.5.
- The color selection in our system is shown in Section 3.6.
- Finally, Section 3.7 describes the positioning method in our system.

## 3.2 Communication Protocol

### 3.2.1 Frame format

In the I-VLCS system, two types of frame format (DATA and ACK) are implemented as shown in Figure 3.2(a) and Figure 3.2(b), respectively. Both frames have a fixed total length for each ModeType; the difference between them is that the ACK frame has no payload segment (length = 0). The maximum payload size is decided by the ModeType of the frame with a pre-defined value. Each frame starts with a three-byte Preamble indicating the beginning of a new frame. ModeType segment represents the mode (Color\_4, Color\_8, Color\_16) which decides the encoding and decoding algorithms used in the current frame. There are four categories of messages used, as shown in Table 3.1: request (REQ), acknowledge (ACK), communication (COM) and calibration (CAL). The REQ and ACK use ACK frame format and the DATA format is used by COM and CAL frame format. The ModeType and the MesType together decide the length of the payload of the frame. The length segment indicates the length of the frame. Source and destination segments store the identifier values. Each device has a unique pre-define identifier value. At the establishing channel stage before communication, the identifier of the source will be sent via REQ frame and stored in the receiver. The receivers will compare the source segment in the current receiving frame with the pre-stored source identifier value to judge whether to decode the received data or drop the frame. A one-byte Cyclic Redundancy Check (CRC) is appended after the payload and the stop segment is attached to the end of each frame.

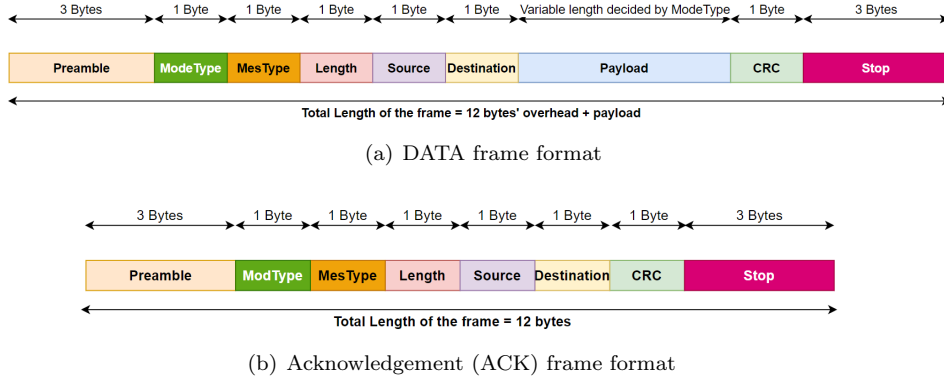


Figure 3.2: The frame format designed in the I-VLCS system

Table 3.1: MesType defined in the protocol

Category	Name	Value	Whether includes the payload
Requese (REQ)	INIT_REQ	0	No
Requese (REQ)	CHAN_REQ	1	No
Requese (REQ)	CAL_REQ	2	No
Requese (REQ)	COM_REQ	3	No
Acknowledge (ACK)	INIT_ACK	4	No
Acknowledge (ACK)	CHAN_ACK	5	No
Acknowledge (ACK)	CAL_ACK	6	No
Acknowledge (ACK)	COM_ACK	7	No
Communication (COM)	COM	8	Yes
Calbration (CAL)	CAL	9	Yes

### 3.2.2 Communication process

The optical LOS channel needs to be established between the transmitter and the receiver for VLC communication. Usually, the LED which has a large beam divergence is considered as a Lambertian source [20]. This, the signals should follow Lambert's emission law i.e., the radiant intensity or luminous intensity, observed from an ideal diffusely reflecting surface or ideal diffuse radiator, is directly proportional to the cosine of the angle between the direction of the incident light and the surface normal [34]. The equation of Lambert's emission law is shown in Equation 3.1 as follows:

$$P_i(\theta, \psi) = \frac{(m_i + 1)A_R P_{T_i}}{2\pi} \cdot \frac{\cos^m(\theta) \cos^M(\psi) T_s(\psi) g(\psi)}{D_i^2}, \quad (3.1)$$

where  $D_i$  is the distance between the  $i^{\text{th}}$  transmitter and the receiver,  $A_R$  is the effective photosensitive area of the receiver component,  $P_{T_i}$  is the optical power of the luminance source,  $\theta$  is the irradiance angle,  $\psi$  is the incident angle,  $T_s(\psi)$  and  $g(\psi)$  are the gain of the optical filter and optical concentrator (lens) placed in front of the detector,  $M$  and  $m$  are Lambertian orders.

However, as with other VLC systems, the RGB LED of the transmitter in the I-VLCS system is packaged with a lens to increase the communication range. The shape and the internal refractive index of the lens have effects on the radi-

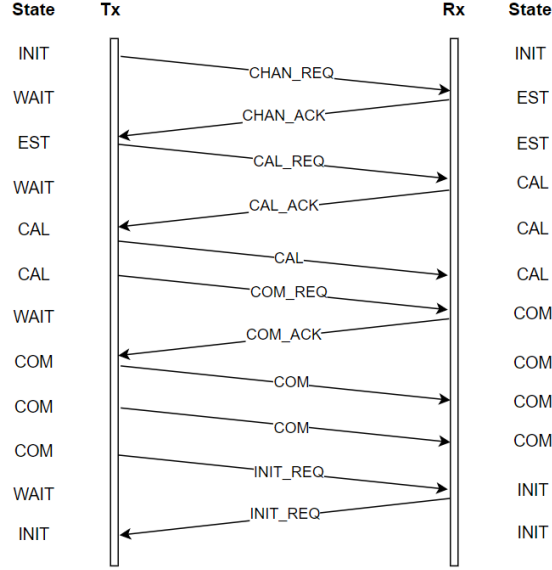


Figure 3.3: **Two-way handshake and communication between the Tx and the Rx**

ation pattern so a new equation considering the lens is required. The researches [43, 42] replaced the classical Lambertian order, optical filter, and concentrator gain with Equation (3.2) for LEDs or PDs packaged with the lens.

$$P_r = (P_t/d^2)C_{opt}G_t(\theta)G_r(\psi) , \quad (3.2)$$

where  $G_t(\theta) = \exp(-\theta_{S_t}/k_t)$  and  $G_r(\psi) = \exp(-\psi_{S_r}/k_r)$ , in which  $S_t$  and  $S_r$  are slope constants affected by the shape of lens.  $k_t$  and  $k_r$  are related to  $\theta_1/2$  and  $\psi_1/2$  by  $k_t = (\theta_1/2)_{S_t}/\ln(1/2)$  and  $k_r = (\psi_1/2)_{S_r}/\ln(1/2)$ .

Figure 3.3 presents the communication processes between a transmitter and a receiver in the I-VLCS system. Both Tx and Rx start from an initial state (INIT) when the power of the device is on. However, the functionality of INIT states of the Tx and Rx are different. At the INIT state, the Tx will keep idle until a command is received from the PC terminal side while the Rx will keep sensing the incoming lights during the INIT state. There are generally two phases for communication:

1. *Channel establishment:* A two-way handshake is implemented to establish the communication channel. The Tx should send a CHAN\_REQ frame to search the target devices when the user inputs the commands to start the device at the PC terminal side. The Tx will change into waiting state (WAIT) in which the RGB LED will be reverse-biased as a photo-detector. The Rx transforms to an established state (EST) as soon as it received the CHAN\_REQ and sent the CHAN\_ACK. Until the CHAN\_ACK frame is received by the Tx, it will change into EST state indicating the channel establishment has been completed.
2. *Communication and sensing:* In this phase, the devices can already communicate and sense with each other via the established LOS chan-

nel. Before activating any new device to start communication or after a device is placed at a new location, the calibration needs to be performed to measure the values for each defined ColorType. Similar with the channel establishment process, the Tx will send CAL\_REQ and change into WAIT state in which the Tx will be a photo-detector device again to keep waiting for the CAL\_ACK frame. The Rx sent the CAL\_ACK back once it received a CAL\_REQ signal and change into CAL state. After the CAL\_ACK is received by the Tx, the Tx will change into CAL state indicating the completion of the calibration between these two devices. During the communication, the Tx keeps sending signals to the receiver, unless it receives the command from the PC terminal side to ask it to change into other states such as re-initialization or re-calibration as shown in Figure 3.3.

### 3.3 Characteristics of Tx and Rx

The characteristics of the Tx and Rx should be measured before determining the ColorType and positioning method used in the system. A concentrator like a lens and the increase of forwarding current through the transmitter LED affects the emitting illuminance directly. The relationship between the communication distance and sensed voltage at the receiver side is closely relevant to our proposed positioning algorithm.

#### 3.3.1 Effects of lens and forward current

Figure 3.4 shows the test results of the light source as the transmitter, in which the solid lines are using simple RGB LED as transmitter and the dotted lines are packaging the emitting LED with a lens in the front. Based on the experimental results, the blue sub LED can emit the highest luminosity among three sub LEDs with the same forward current. Packaging the lens in front of the RGB LEDs has a significant influence on the luminous which can improve the quality of the communication and sensing.

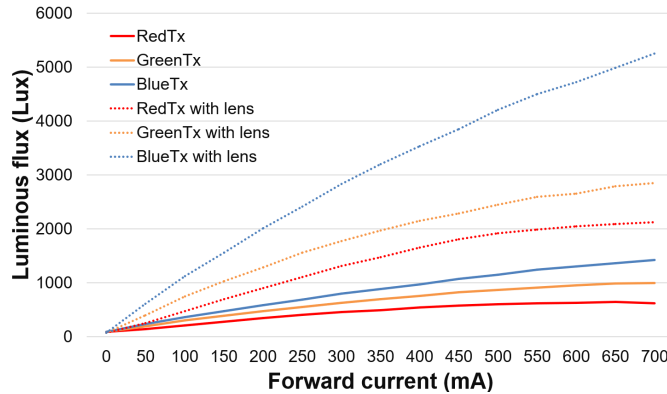
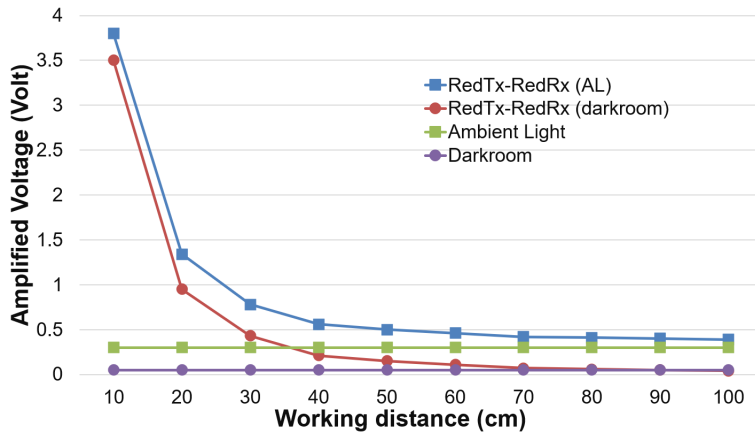
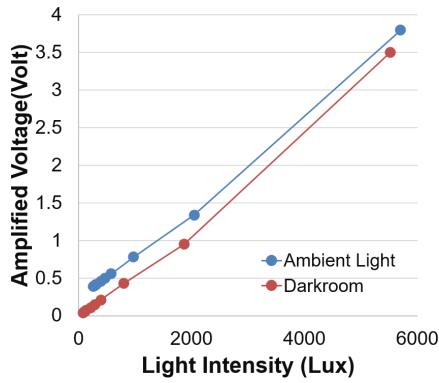


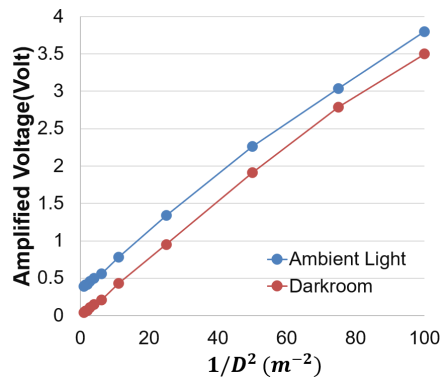
Figure 3.4: Relationship between the luminous flux and forward current through the Tx RGB LED



(a) Voltage and communication distance



(b) Voltage and light intensity



(c) Voltage and 1/D<sup>2</sup>

Figure 3.5: The effects of distance and light intensity at the Rx LED surface on the sensed photoelectric voltage

Although most IoT devices do not package with the existing LEDs with the lens, the Tx LED with a lens is taken in the I-VLCS system to improve the communication distance and communication accuracy after massive experiments.

The generated luminosity increases slower when the forward current is higher because of the increase in the temperature of the transmitter. The selected LED accepts the absolute maximum forward current of 700 mA but the Tx device will achieve a very high temperature after working several minutes with the 700 mA forward current which is much higher than the tolerated temperature (40 degrees) of the lens. After the trade-off based on the measurements, the maximum forward current through the Tx LED in the I-VLCS system is 350 mA.

### 3.3.2 Effects of distance and light intensity

The effects of the communication distance and light intensity received at the Rx LED surface on the sensed photoelectric voltage is present in Figure 3.5

which presents the voltage read at pins of the Rx with the increase of the communication range between the Rx and the Tx, in which the red and blue lines are the sensed values by the red sub LED with the red incoming lights under the darkroom and ambient lights environment respectively and the green and purple lines are the detected voltage values without incoming signals. We can see that the ambient light has a negligible effect on the communication under the RedTx-RedRx combination.

Figure 3.5(b) and Figure 3.5(c) present the sensed voltages of the red sub LED with the red incoming lights in which the blue line is the data measured under the ambient light environment and the red line is measured in the darkroom. The generated photo-currents of an ideal photo-detector should be linear with the received light intensity on its surface. The experimental results in Figure 3.5(b) prove that the Rx in the I-VLCS system can be seen as an ideal photo-detector. The generated photoelectric current is linearly amplified and converted into the voltages read by the Rx, and the reading voltages are linear with the light intensity at the Rx surface measured by the illuminance meter. Besides, the Figure 3.5(c) indicates that the reading voltages values by the Rx are linear with the reciprocal of the square of the communication distances  $D$  following the Equation 3.5, which is an important prerequisite to implement our positioning methods. That means we only need to consider the angles at the on-line positioning phase, and the distance can be estimated by the voltage values of each ColorType.

### 3.4 Responsivity

The responsivity  $R$  is a parameter indicating the sensitivity of the photo-detector, which is the fundamental of the communication in the I-VLCS system. It is defined as the magnitude of the photo-current  $I_p$  produced relative to the incident optical power  $P_o$  received on the photosensitive area of the photo-detector:

$$R = \frac{I_p}{P_o} . \quad (3.3)$$

The higher the responsivity  $R$  of a photo-detector means it has a better response. The responsivity is related to the wavelength of the incident light and the type of sub-LEDs as Rx, which is the key factor used for recognizing the color of the incoming lights on the Rx during the RGB LED to LED communication in the I-VLCS system. Besides, the greater reverse bias voltages on the photo-detector and the increase of the photosensitive area can achieve a higher responsivity as well, so we control each sub-LEDs of the Rx working at the same reverse-biased voltages while communicating.

The responsivity measured for the RX RGB LED is shown in Figure 3.6, in which the Figure 3.6(a) includes all the nine possible Tx-Rx color combinations (e.g., the RedTx - RedRx representing the voltages read by red sub-LED with the red incoming light generated with the maximum measured forward current 350 mA at the Tx red sub-LED). Among three sub-LEDs, the blue sub-LED has the best performance working as a photo-detector which has the highest responsivity to the blue incoming lights, a medium responsivity to the green incoming lights, and a low response to the red incoming lights. RedTx-RedRx has quite good responsivity as well as expected, which is the most widely used

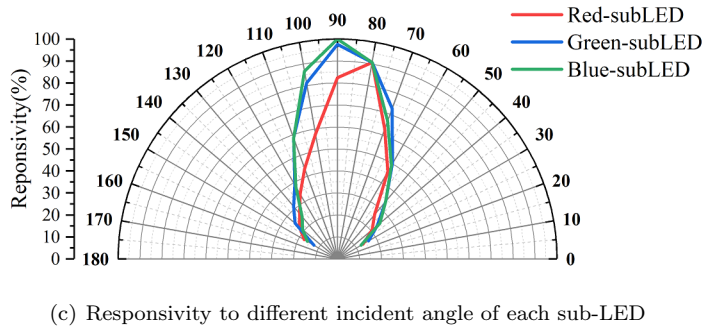
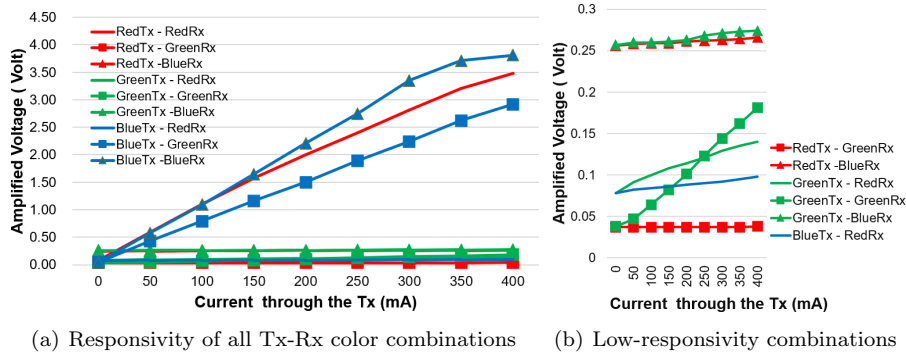


Figure 3.6: The responsivity of the RGB LED as the photo-detector

combination for LED to LED communications. However, the green sub-LED has a very low response to all the incoming lights even hardly distinguishing between the ambient light and incoming signals which makes it is not suitable as a photo-detector. To perform the color recognition in the I-VLCS system, we have to choose 4, 8, 16 Tx-Rx color combinations which can be distinguished by the photoelectric voltages of three sub-LEDs which will be introduced in Section 3.6. Because of the distribution of each sub-LED encapsulated in the chosen RGB LED, the characteristic of angular responsivity of each sub-LED is shown in Figure 3.6(c). The distance to the center of the semicircle represents the responsivity in percent which is defined as the ratio of measured voltage of current angle  $V_c$  to the maximum voltage  $V_{max}$  achieved for the sub-LEDs among all measure angles:

$$R_a = \frac{V_c}{V_{max}} . \quad (3.4)$$

The Red sub-LED, Green sub-LED and Blue sub-LED are measured under their best color combinations that are RedTx-RedRx, BlueTx-GreenRx and BlueTx-BlueRx respectively based on the previous test results from Figure 3.6(a). The measured angular responsivity indicates that the angle reaching a maximum responsivity for each sub-LED are different due to the encapsulation of the LED, the angles with the maximum responsivity for R, G, B sub-LEDs are  $80^\circ$ ,  $90^\circ$ ,  $90^\circ$ , respectively.

Table 3.2: **Coding Scheme for Color\_4 ModeType**

<i>ColorType</i>	<i>RedTx(mA)</i>	<i>GreenTx(mA)</i>	<i>BlueTx(mA)</i>	<i>Binary</i>
color1Tx	350	0	0	00
color6Tx	0	350	0	01
color11Tx	0	0	350	10
color12Tx	350	350	350	11

Table 3.3: **Coding Scheme for Color\_8 ModeType**

<i>ColorType</i>	<i>RedTx(mA)</i>	<i>GreenTx(mA)</i>	<i>BlueTx(mA)</i>	<i>Binary</i>
color1Tx	350	0	0	000
color3Tx	200	0	0	001
color5Tx	50	0	0	010
color6Tx	0	0	350	011
color8Tx	0	0	220	100
color11Tx	0	350	0	101
color12Tx	350	350	350	110
color14Tx	200	200	200	111

## 3.5 Coding Scheme

Compared with the VLC system using single-color LEDs, transmitters deployed in the I-VLCS system take one ColorType as a basic unit instead of the bit stream. The bits in the data are encoded into the corresponding color sequence depending on the ModeType of the frame. Theoretically, the I-VLCS system should have higher data rates compared with single color LED-to-LED communication at the same transmitting frequency because each transmitted color in the sequence can represent multiple bits. Usually, the exhaustion searching method is used in classical coding schemes of pulse position-based modulation schemes such as tabulation and constellation approaches [33, 30].

### 3.5.1 Encoding

We propose a coding scheme specially for the I-VLCS system as shown in the following tables. RedTx, GreenTx and BlueTx represent the current through the sub LED to generate the corresponding color light respectively. The chosen values are based on the experimental results carefully because the noise caused by temperature and limitation from hardware design has a significant impact on communication and positioning accuracy which will be introduced in Chapter 5.

In Color\_4 ModeType frames, four colors are determined and each color represents two binary bits as shown in Table 3.2. The color1Tx, color 6Tx, color11Tx and color 12Tx are selected for Color\_4 ModeType frames which are the maximum current (350 mA) used for emitting in our system through each sub-LED and their mixed emitting light respectively. Similarly, the colorType used for Color\_8 ModeType and Color\_16 ModeType are present in Table 3.3 and Table 3.4. We can see that there are generally four types of colors used for emitting without considering the brightness, red, green, blue, and the mixed light of three sub-LEDs. These combinations chosen are based on massive experiments about their responsibility and stability which achieve the highest accuracy in the testbench of communication. The corresponding experimental

Table 3.4: Coding Scheme for Color\_16 ModeType

<i>ColorType</i>	<i>RedTx(mA)</i>	<i>GreenTx(mA)</i>	<i>BlueTx(mA)</i>	<i>Binary</i>
color1Tx	350	0	0	0000
color2Tx	275	0	0	0001
color3Tx	200	0	0	0010
color4Tx	125	0	0	0011
color5Tx	50	0	0	0100
color6Tx	0	0	350	0101
color7Tx	0	0	275	0110
color8Tx	0	0	200	0111
color9Tx	0	0	125	1000
color10Tx	0	0	50	1001
color11Tx	0	350	0	1010
color12Tx	350	350	350	1011
color13Tx	275	275	275	1100
color14Tx	200	200	200	1101
color15Tx	125	125	125	1110
color16Tx	50	50	50	1111

results showing the reason for choosing these colors and current values will be presented in detail in Chapter 5. The single green sub-LED emitting light as the transmitter is only used once in all three ModeType because all three sub-LEDs have quite a low responsivity to green incident light which is even hardly distinguished from the ambient light reading. This means the green light is not suitable as a parameter for color recognition in the decoding process.

During the encoding process, the encoding algorithms in the Tx will first check the mode type segment of the frame. Then the data will be encoded into color sequences based on the corresponding coding scheme. An interrupt will be triggered when the end of the frame is checked, then the ISR will set the pre-defined GPIO for each color detected in the sequence as high voltage to drive the RGB LED. After transmitting a frame the transmitter will check the current state to decide to transmit the next frame or wait for the incoming signal such as ACK MesType for channel establishment sent by other devices.

During the decoding process, the three sub-LEDs of the RGB LED as photo-detector will generate photo-currents respectively due to their difference responsivity to the color of incoming lights. The currents will be amplified and converted into voltage values through the TIA circuit which will be stored in the buffer of the receiver until the end of the frame. The MCU will perform color recognition based on the database collected in the calibration stage for the frame stored in the buffer and decode the color sequence which will be converted into the binary bits next based on the ModeType detected in the frame. According to the MesType of current received frame and the state of the receiver, the receiver will keep reverse-biasing the RGB LED as a photo-detector or forward-bias the RGB LED to send messages to other devices.

### 3.5.2 Decoding

There are three process of decoding the incoming values at pins at the Rx: calibration, color recognition and decoding.

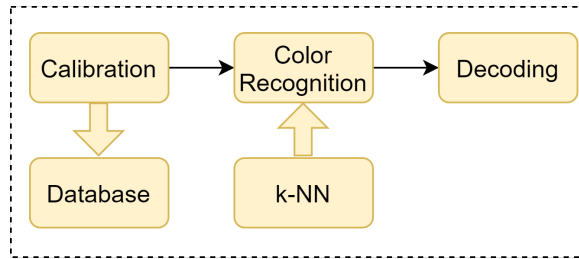


Figure 3.7: **Decoding process**

1. *Calibration:* The calibration step calibrates the values of each defined ColorType. The payload in the frame with Calibration MesType consists of the fixed color sequences. The color in the calibration sequence starts with the Color 1Tx and follows with this fixed sequence circularly so each ColorType can be sampled multiple times. The sampled values of each ColorType are stored in the database for further color recognition.
2. *Color recognition:* The color recognition process is to classify the sensed values into the corresponding clusters representing each ColorType. The k-NN algorithm is used to classify the color of incoming signals. The Euclidean distance between the current sensed value and each data of ColorType is calculated and the incoming signal will be classified into the cluster that reaches the pre-defined  $K$  values. If the detected signals reach the  $K$  values in more than one cluster, the sum of the distances will be compared and the signal will be classified into the ColorType with the minimum sum distance.
3. *Decoding:* When the data in the frame is classified as a ColorType during communication, each ColorType will be decoded into binary bits based on the coding scheme and the ModeType of the frame. For example, each color of the frame with the Color\_4 ModeType (color1Tx, color6Tx, color11Tx and color12Tx) will be decoded into 00, 01, 10, 11, respectively. The sequence of colors will be converted into binary bits for further measuring the features such as communication accuracy, etc.

### 3.6 Color Selection

The final selection of the chosen 16 ColorType and their measurement results are shown in Figure 3.8 based on the tested responsivity of each Tx-Rx combination and the proposed coding scheme. The results are measured with the 1000 Hz transmitting frequency in the normal indoor ambient light environment. From color1Tx to color5Tx are the generated red lights from the Tx LED with different forward bias current through the Tx LED, similarly, from color6Tx to color10Tx are visible blue lights, color11Tx is the green lights, the rest are the mixed colors of three emitting lights from sub-LEDs. Based on the characteristics of the responsivity to incident lights with different wavelengths (colors) and the results tested in Section 3.4, the Rx can classify the ColorType of the incoming signals. For example, The Rx should get quite high values at

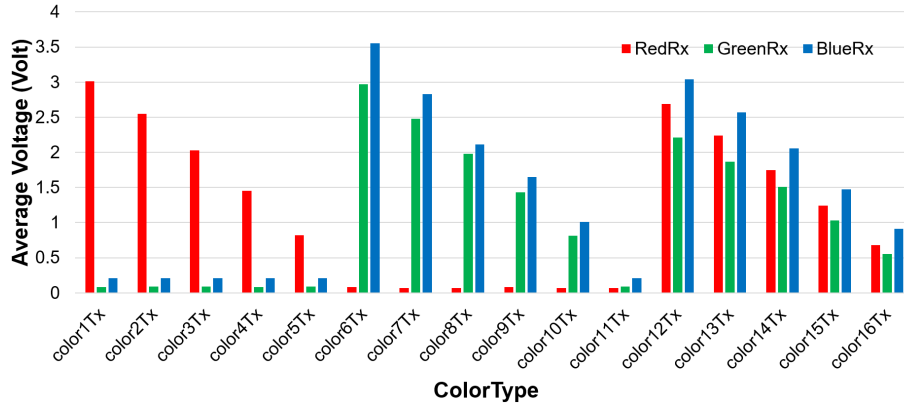


Figure 3.8: Selected ColorType for Color\_16 Mode

Red sub-LED and small values for the rest two sub-LEDs for a red ColorType, the pre-collected database at the calibration stage before communication, and the difference between the selected Tx lights are handled next to further distinguish the ColorType of the incoming signals. From color12Tx to color16Tx are the mixed lights which are white from human eyes, all three sub-LEDs have a good response to the chosen mixed lights. The color1Tx, color6Tx, color11Tx and color12Tx are used for Color\_4 ModeType frames, and color1Tx, color3Tx, color5Tx, color6Tx, color8Tx, color11Tx, color12Tx, color14Tx are selected for Color\_8 ModeType frames for the coding scheme based on the experimental results that these combinations having the best performance.

### 3.7 Positioning Method

For positioning the target device, we propose an algorithm based on the RSS model which can estimate the two-dimensional location of the Tx under the Rx's coordinate using only one pair of RGB LED.

Ideally, the photoelectric current of the RGB LED as the photo-detector should follow the relations between the intensity of light and the photo-current as an ideal photo-detector, that is the photoelectric current increases linearly with an increase in the intensity of incident light. The relationship between the illuminance and distance follow the Equation (3.5):

$$E = I/D^2, \quad (3.5)$$

where  $E$  is the illuminance emitted by the light source (Tx LED),  $I$  is the luminosity (in lumens) of the source and  $D$  is the distance between the surface of the source to the receiver.

There are two phases of our positioning algorithm: offline collection and online positioning. The offline phase is to collect the data to generate the estimation equations to position the target device, during which the Tx will send a calibration frame to the Rx to sense the digital values of each sub-LED of the three selected color combinations at every test location. The experimental setup of the off-line phase is shown in Figure 3.9, the semicircle in front of the

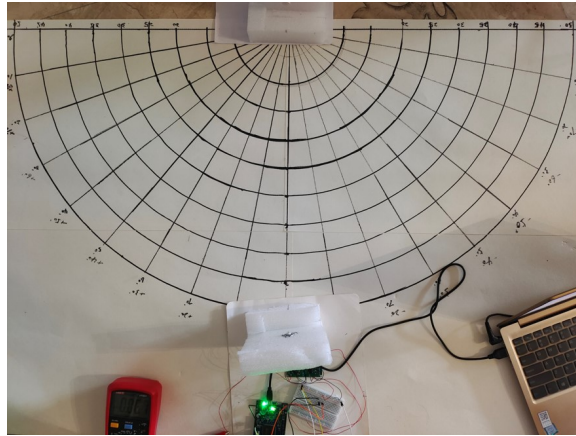


Figure 3.9: **Experimental setup of positioning**

Tx is divided into multiple test grids. The concentric semicircles between the Tx and Rx divide the distances from 0 cm to 50 cm into 10 intervals equally, the distance between every two concentric semicircles is 5 cm. Meanwhile, the lines originating from the center of the semicircle divide the semicircle with the same angular intervals (10 degrees). The intersections of lines and concentric semicircles divide the field in front of the Rx into 180 grids. While the actual number of the test grids used is less due to the limited field of view of the RGB LED as the photo-detector and the pressure of intensive labor work. The actual number of test grids is 65 which is present in Section 5.4.

For each incoming light, the RGB LED at the Rx side will receive 3 values from each subLED respectively at each test location. The Rx need to locate the distance and the angle of the Tx based on the incoming lights, in which there are two parameters that need to determine so it needs to have at least two equations to calculate the distance and angle theoretically. The final selected combinations are decided by the measurements: RedTx-RedRx, BlueTx-GreenRx and BlueTx-BlueRx, in which the former part (e.g., RedTX) is the color of the incoming light generated by 350 mA forwarded current and the latter part (e.g., RedRx) is the color of the selected sub-LED. The collected data is sent to the PC and used the MATLAB curve fitting tool to generate three equations below:

$$V_{RR} = f_1(\theta, d) , \quad (3.6)$$

$$V_{BG} = f_1(\theta, d) , \quad (3.7)$$

$$V_{BB} = f_1(\theta, d) , \quad (3.8)$$

where  $V_{RR}$ ,  $V_{BG}$ ,  $V_{BB}$  are the sensed voltages for RedTx-RedRx, BlueTx-GreenRx and BlueTx-BlueRx combinations respectively, and  $\theta$  is the relative angle of the Tx under the Rx's coordinate and  $d$  is the distance between the Tx LED and Rx LED. Due to the linear relationship between the distance and the photo-current is proved in our system in Chapter 5, we only need to estimate the angle parameter of Tx in the Rx's coordinate when positioning at the online phase. The details of the measurements and results are present in Chapter 5.

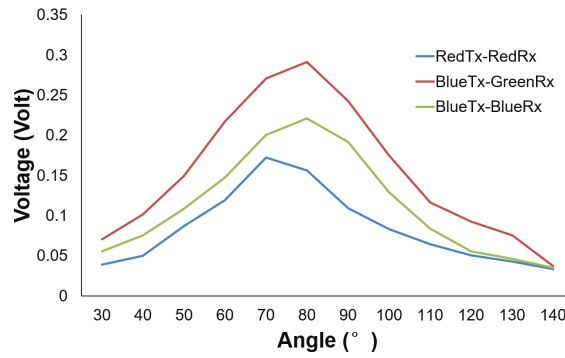


Figure 3.10: **The three Tx-Rx combinations selected for positioning**

After the off-line phase, each Rx will get three equations and it can calculate the relative distance and angle based on the sensed values of selected combinations when receiving the POS\_REQ command from the PC terminal during the normal VLC communication. The selected color in the payload of the DATA frame will be checked by the Rx and the values of each combination will be read and used to estimate the relative position of the current Tx device.



## Chapter 4

# Implementation

This chapter presents the implementation of the proposed I-VLCS system with RGB LEDs. An overview of the system implementation is given in Section 4.1, followed by the hardware and the software implementation details introduced in Section 4.2 and Section 4.3, respectively.

### 4.1 Overview

Figure 4.1 presents the high-level overview of the implementation of our proposed I-VLCS system with RGB LEDs. The embedded board handles all the software implementations including encoding/decoding, modulation/demodulation and positioning. The embedded board used in our project is the 32-bit core MCU called Arduino Due based on Atmel SAM3X8E ARM Cortex-M3 CPU, as shown in Figure 4.2. The reasons that Arduino Due is chosen for our system implementation are listed as follows:

1. *Small scale:* our I-VLCS system targets at the small IoT devices so it is important to simulate small-size IoT devices without any input and output peripherals such as a keyboard or a display. Arduino Due is quite small with 101.52 mm length and 53.3 mm width [1].
2. *Easy to prototype:* Arduino Due has 54 digital GPIO pins of which 12 can be used as PWM outputs and 12 for analog inputs, making it convenient for prototyping and designing a system. Arduino Due features up to 512 KB flash memory, which is available for writing user applications via USB using the specific Arduino IDE.
3. *High computation ability:* Arduino Due is embedded with a high-performance 32-bit ARM Cortex-M3 core (SAM3X8E) with a maximum speed of 84 MHz, which is enough to meet with the computing requirements of positioning and color recognition of our system.
4. *Cost-efficiency:* Arduino Due is a cheap (about 35 euros) and an off-the-shelf embedded board that can purchase easily.

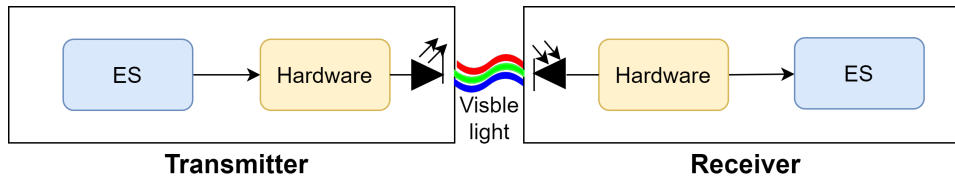


Figure 4.1: A high-level overview of the system implementation

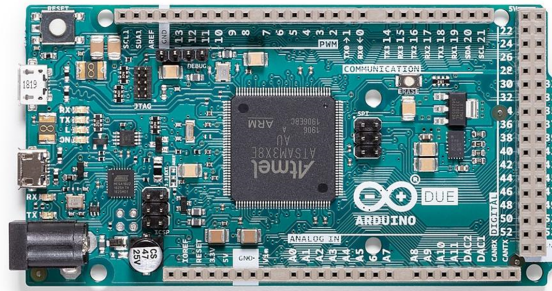


Figure 4.2: Arduino Due embedded board [1]

## 4.2 Hardware Implementation

The general architecture of the hardware is given in Figure 4.3. There are mainly four parts: the PC terminal side in blue rectangles, the communication channel represented by the orange color, and the Tx block on the bottom left and the Rx block on the bottom right of the figure respectively.

The PC connects with both Tx and Rx via the USB serial port through which the user can easily send commands to devices on the user interface. The flash of the MCU in Arduino Due is used for storing codes of application. The 32-bit processor should generate data and encode it into frames based on the commands received from the USB serial port. The MCU encodes the binary bits in the frame and then controls the RGB LED emitting the corresponding sequence of lights through the driver circuit. At the receiver side, the RGB LED is reverse-biased and keeps receiving the visible light signals. These signals will be amplified and converted into voltages through the Trans-Impedance Amplifier (TIA) circuit. Then the signals will be converted into digital values by the inbuilt Analog-to-Digital Converter (ADC) in the Arduino Due after filtering. After that, the color recognition is performed based on the data collected in the calibration stage. During the experiments, the relevant data such as the generated frames sent by the Tx and the decoded binary sequences by the Rx can be easily obtained by the user at the PC terminal by sending a command to the Rx via the USB serial port. Based on these data, the key parameters of the I-VLCS system can be easily calculated for evaluation and debugging.

### 4.2.1 Transmitter

In our project, we have explored the off-the-shelf high-power RGB LED and low-power RGB LED as the emitting device as shown in Figure 4.4(a). A low-

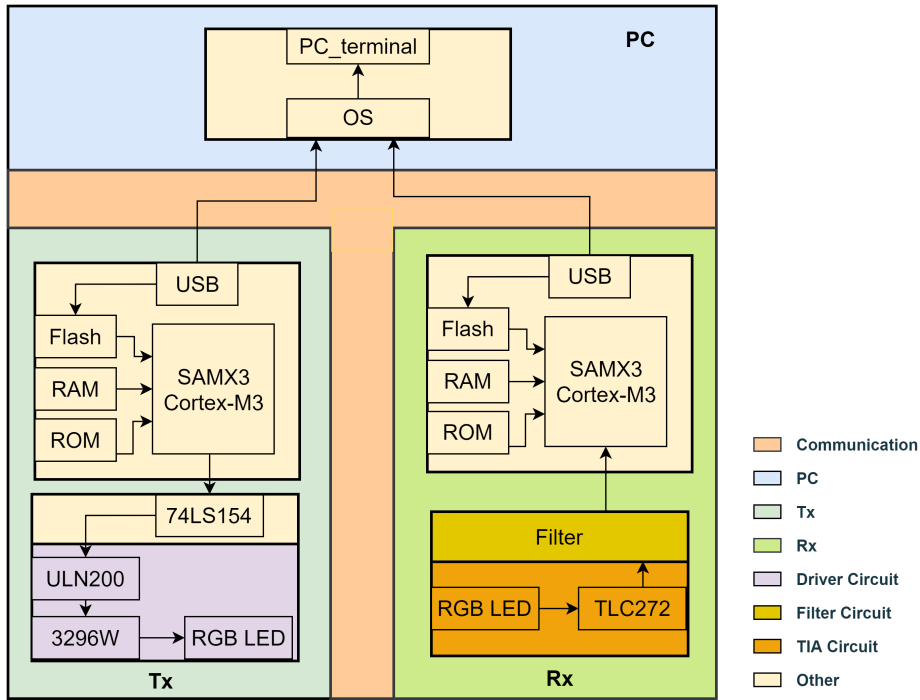


Figure 4.3: Block diagram of the overall hardware implementation

power RGB LED was selected as the photo-detector in the I-VLCS system at the beginning which can be driven directly by the GPIO outputs voltages and controlled its brightness using Pulse-Width Modulation (PWM) signals. The chosen low-power RGB LED for testing is a 5mm LED YSL-R596CR3G4B5C-C10 with a 20 mA working forward current a 5-volt forward voltage. However, the low power of emitted light makes it have a quite short communication range. The maximum communication distance at which a high communication accuracy can be achieved by the low-power RGB LED measured in the experiments is approximate 6 cm, which is definitely not enough in most application scenarios.

Due to the limitation of the low-power RGB LED mentioned above, we instead explore a high-power RGB LED (JH-9RGB14G45-S2A-M), which has a 700 mA

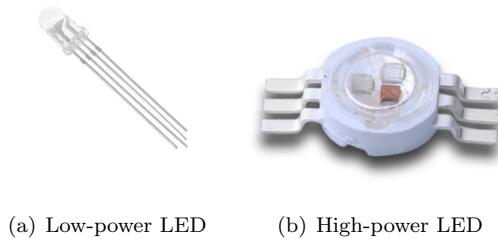


Figure 4.4: RGB LEDs tested in the project

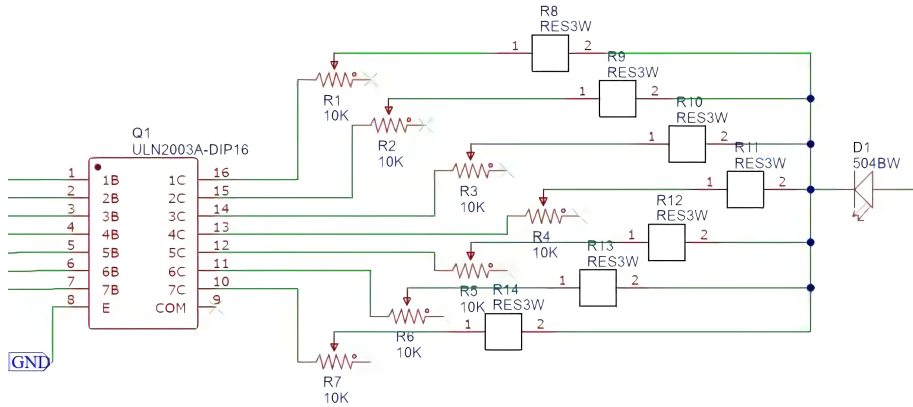


Figure 4.5: The driver circuit of the Tx

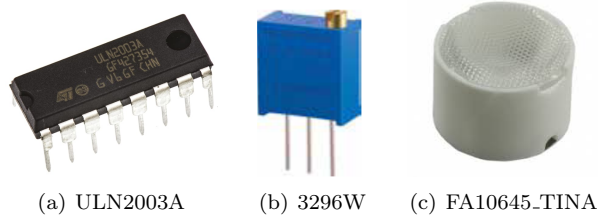


Figure 4.6: Some of the electronic devices used in the Tx

rate current for every sub-LED of R/G/B, as shown in Figure 4.4(b). The GPIO of the embedded board does not have the ability to drive such a high-power RGB LED directly. Thus, a 12-volt external power source is added.

The schematic of the final design of the Tx driver circuit is shown in Figure 4.5. The ULN2003A, as shown in Figure 4.6(a), is a high-voltage, high-current Darlington transistor array consisting of seven NPN Darlington pairs which are used to increase the drive ability of the controller to light up the RGB LED. Each sub-LED connects with one ULN2003A device which receives the signals from the MCU via pins 1–7. Each channel of the ULN2003A device consists of Darlington connected NPN transistors to simulate a switch to control the brightness of each sub-LED. For example, the channel between pin 1 and pin 16 is on if a signal is received on pin 1, the RGB LED will get a fixed forward current for emitting the corresponding color which is configured before. The rest of the relevant components used in the Tx are shown in Figure 4.6. The trimming potentiometer 3296W in Figure 4.6(b) is used to control the forward current through the LED.

A lens (FA10645\_TINA), as shown in Figure 4.6(c), is placed in the front of the RGB LED to further increase the communication range in the system. Ideally, the brightness of an expected LED transmitter has a linear function of forwarding current. As mentioned in Section 3.2.2, the optical concentrator and the shape of the lens both are key factors in the Lambert equations, which means the radiation pattern and the optical characteristic of the RGB LED packaged

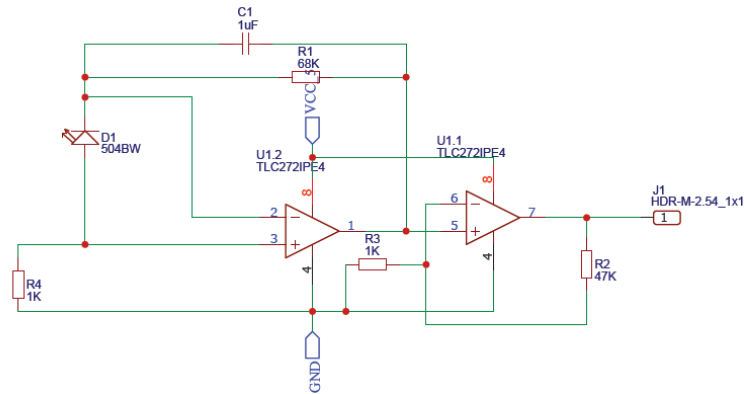


Figure 4.7: Schematic of the Rx

with a lens should be different comparing the single RGB LED as an emitter. Besides, the other characteristic of the emitting devices such as the volt-ampere characteristics and optical characteristic curve are tested in Chapter 5.

#### 4.2.2 Receiver

The implementation of the receiver follows the typical VLC receiver design, which is generally composed of five parts: photodetector, amplifier, filter, ADC, and MCU. The receiver works as a simple visible light sensor to demodulate incoming signals into the sequences of colors which will be decoded into binary bits next.

Typically, incoming light signals are sensed by the reversed RGB LED as the photo-detector first, and corresponding photo-currents will be generated. Both low-power and high-power RGB LEDs mentioned above are measured in Chapter 5. The experimental results show it has a quite low responsivity to incoming lights which means the photo-current is quite small. The currents are amplified and converted into voltages through the TIA circuit next meanwhile the noise is amplified as well, which leads to difficulty in the color recognition and decoding of incoming signals using the reverse-biased low power RGB LED as the photo-detector. Except that, the low-power LED has a narrow FOV resulting in it can merely sense the incident lights within a limited field of angles. Hence, it is also a disadvantage to implementing the positioning and sensing functionality at the receiver side with the low-power RGB LED. The three sub-LEDs of the high-power RGB LED have a good responsivity and better FOV based on our experiments, which is reversed biased as a photo-detector in the I-VLCS system. A simple RC filter is implemented in the system before signals are amplified by the amplifier. The TIA circuit of the receiver is shown in Figure 4.7, in which the TLC272 is used as the amplifier in the I-VLCS system. TLC272 is a dual operational amplifier that is designed as the TIA circuit to amplify and convert the input photocurrent into voltages. The maximum acceptable input voltage on GPIO of the inbuilt ADC of Arduino Due is 3.3 volt which means we have to control the amplified voltages meanwhile making them easy to classify and recognize by MCU as possible to guarantee the high accuracy of the data during communication. Our system does not achieve a very high

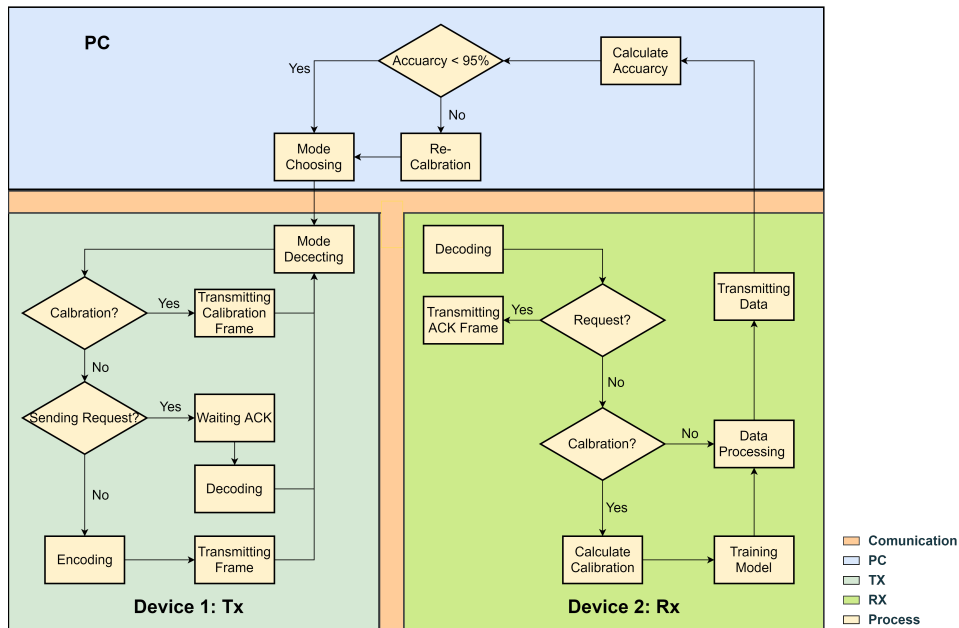


Figure 4.8: **Software implementation**

transmitting frequency and the built-in ADC is faster enough for the sampling process in experiments. The MCU samples the input signals and converts them into digital values which will be decoded next.

### 4.3 Software Implementation

The overview of software implementation of the I-VLCS system is shown in Figure 4.8, which are consisted of four parts: PC, Tx, Rx and communication channel. Both Tx and Rx can communicate with PC via USB.

After writing the applications in MCUs, the PC can choose a mode on the user interface. The user can choose to generate random data or input the specific data as the payload of the frame via the serial port. After the mode is determined, the PC will send a value representing the selected mode. Then the Tx detects the mode to determine the ModeType and of the frame. If the mode is calibration mode, a DATA frame will be generated with the pre-defined data representing a fixed sequence of the light colors. If the model needs to generate an ACK frame to send a request message, the PC will not send any data. The value of mode choosing send by the PC decides the MesType of the ACK frame, and the Tx will change into waiting states until receiving the corresponding ACK frame. If the mode is communication, the PC will send the data as the payload to generate the frame.

The receiver starts to receive the messages once it is powered on. Arduino Due has inbuilt ADC and functions such as analogRead() and digitalRead() which are used to read the input signals generated by the incoming lights at input pins while both functions take up to 100 microseconds. To guarantee the communication and sensing quality of the system, the Rx needs to sample

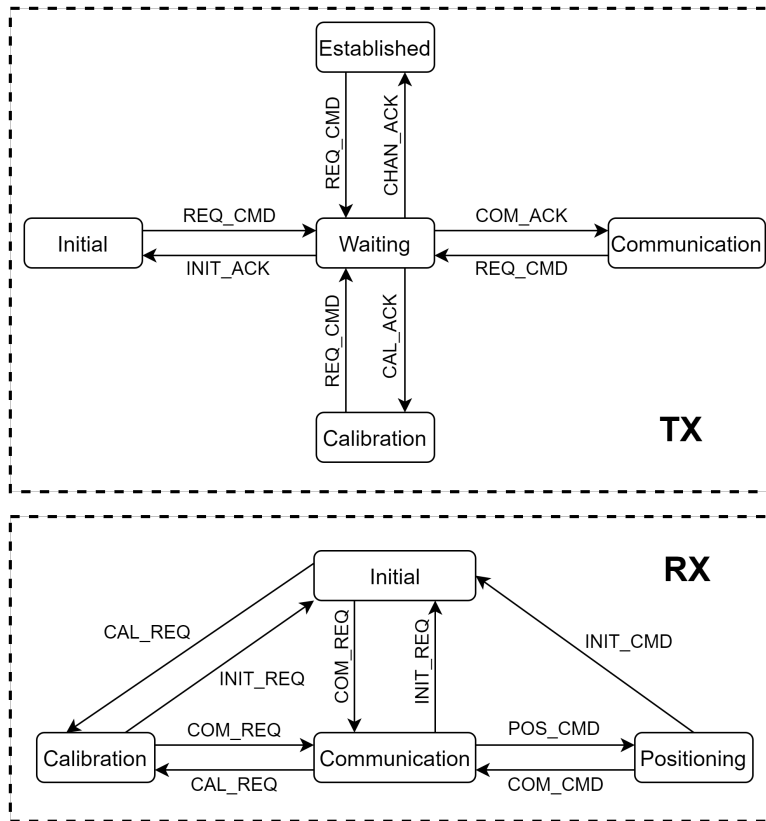


Figure 4.9: Finite-state machine (FSM) of Tx and Rx

multiple times according to the sampling theory. Hence, the transmitting rate is limited in the I-VLCS system. The Rx will keep using the `analogRead()` function to convert signals into digital bits and compare their preamble, source, and destination. When the expected message is received after checking the Source and Destination segments are matched, the Rx will check the binary sequences in `MesType` and `ModeType` next. The `MesType` decides how to handle the message and the `ModeType` decides the decoding algorithms. If it is a request message, the Rx will transmit the ACK frame back. The sequence of the colors in the payload of a calibration frame is known, so the Rx can detect the sensed values of each color of each `ColorType` and store the data in the database for the further color recognition process. If the message is a communication frame, the Rx will recognize the sequence of the colors based on the collected database and decode the data next. During the experiments, the decoded data will send back to the PC terminal and be compared with the original data to check the accuracy bit by bit. If the accuracy is lower than a pre-defined threshold value, for example, there is an obstacle at the light of sight channel or the devices are moved to a new location, the I-VLCS system will ask the devices to perform re-calibration to guarantee successful communication.

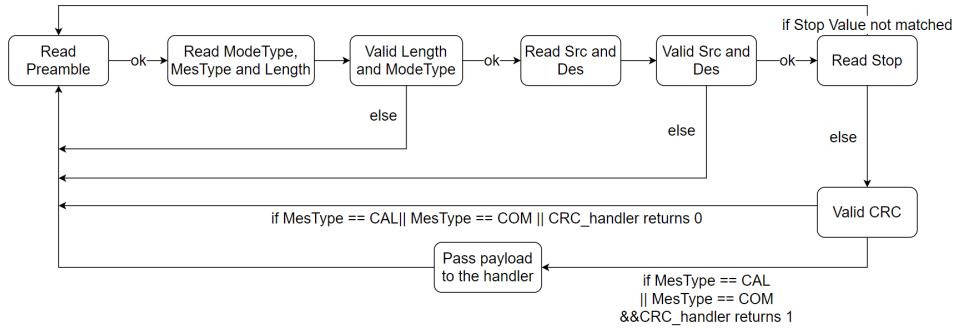


Figure 4.10: FSM of serial communication

## 4.4 Finite-state machine (FSM)

### 4.4.1 FSM of Tx and Rx

The FSM of Tx and Rx in the I-VLCS system is presented in Figure 4.9. There are five states in both Tx and Rx and four of them have the same name but different meanings. The five states in the Tx are initial (INIT), waiting (WAIT), established (EST), calibration (CAL) and communication (COM). The initial state is the beginning state of the Tx when it is given electrical power, in which the Tx keeps waiting for the command from the PC terminal. Once any command or REQ frame is received by the transmitter, it turns into the waiting state in which it waits for the corresponding ACK frame to transfer into the next state. The Tx will move to the established state which is for setting up the LOS communication channel when receiving the CHAN\_ACK frame at the waiting state. Similarly, the Tx should transform into calibration state and communication state when receiving the CAL\_ACK and COM\_ACK frames respectively at the waiting state.

As for the Rx, there is no waiting state but a positioning (POS) state is added. The Rx will change into the corresponding state when receiving the different REQ frames. For example, a CAL\_REQ is detected by the Rx when it is at the communication state and the Rx will change into the calibration state next. While receiving the REQ frames will not work if the transform between two states is forbidden. Besides, the Rx can easily move to the positioning state by being given a POS\_CMD command to estimate the location of the target device based on the selected ColorType used for positioning in the current frame and the formula of the fitting curves generated during calibration. More details about the states of the Tx and Rx can be found in Appendix A.

### 4.4.2 FSM of serial communication

Figure 4.10 presents the FSM of the serial communication process in our I-VLCS system. After the communication channel has been established, the receiver will keep checking the data until a preamble segment is checked during communication. Once a preamble is checked, the MCU will check the ModeType, MesType, and Length segments to determine the mode, message type and length of the frame. In this step, the receiver compares the length read from the Length

```

COM7
Average color R for color1Input the keys for the IVLCS:
*****;
q - calibration:
w - communication with random data
e - communication with specific data
p - print the current calibration values of each color
s - stop
c - clear the database and the buffer
*****;
p
Arduino Matched: p
*****;
Average color R for color1 is: 1097
Average color G for color1 is: 57
Autoscroll Show timestamp Newline 115200 baud Clear output

```

Figure 4.11: User interface of the Tx

segment and the length inferred from ModeType and MesType. If the length of the received frame is accurate, the identifiers of source and destination will be checked otherwise the frame will be dropped. After checking the identifiers, the receiver will check the stop and CRC of the frame. If all the steps mentioned above have been done, the frame will read the payload if it is a DATA frame and pass the payload to the handler for decoding. Or the receiver will change its state depending on the MesType received if it is an ACK frame.

#### 4.4.3 User interface

Simple user interfaces for both Tx and Rx are designed for the I-VLCS system, by which the user can send the command to control the device directly. The user interfaces simply use the serial port in the Arduino IDE to present the available sections and read the input data in the buffer. Figure 4.11 is a part of the Tx user interface, in which the user can input the values from the keyboard to easily control the expected functionality of the devices such as calibration, communication, stop, etc. There is a similar UI for the Rx as well, in which the user can send the POS\_REQ to ask the Rx to estimate the relative locations of the light source, the results can be printed in the interface for evaluating the accuracy of the positioning and debugging in the experiments.



## Chapter 5

# Performance Evaluation

This chapter presents the experimental evaluations of the proposed I-VLCS system. The performance of the system is evaluated in Section ?? and the possible reasons of the noise and errors are discussed in Section 5.2.

### 5.1 Experimental Setup

The experimental setup is shown in Figure 5.1. The left part is the transmitter and the right part represents the receiver. The RGB LEDs on MCU at both Tx and Rx devices are installed in a plastic platform that keeps the same height to the desktop during the experiments. The Arduino connects with the Tx PCB to control and transmit the color sequence to the Rx. On the receiver side, we also design an Rx PCB including a TIA circuit and filters to amplify sensing values of the reverse-biased LED to the MCU for color recognition.

For the experimental tests, there are mainly three steps:

1. The first step is setting up the communication channel according to the protocol that is present in Section 3.2. Due to the Tx being packaged with a lens, the Tx LED and Rx LED have different responsivity for the same incoming light.
2. Calibration needs to be done before starting communication using a new device or located in a new position for collecting data into the database. The Tx will send a DATA frame with a fixed color sequence which is known by the Rx. The Rx will read the sensing values for each ColorType of incoming lights. The Tx sometimes needs to receive an ACK frame sent by the Rx which is usually much simple and the data is pre-defined in the Tx software.
3. During the communication, the Rx will keep listening to the incoming signals. The user can control the Tx to transmit random frames like we do in evaluation or send a specific frame through the user interface designed in IDE. The interface is simple which reads the pre-defined key values inputting from the keyboard in the buffer of the serial port to perform the corresponding functionality like re-calibration, stop communication, etc.

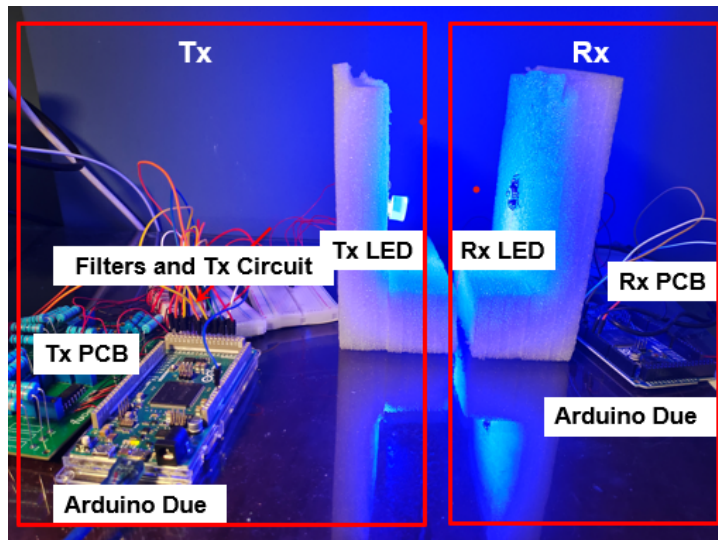


Figure 5.1: **Experimental setup**

## 5.2 Noise Measurement

Signal-to-Noise-Ratio(SNR) is essential to evaluate the performance of a VLC system. Thus, the measurements of noise in an LED-to-LED communication system is necessary. The digital values for the same incoming signals vary a lot as shown in Figure 5.2. For example, the maximum value of sensed voltages reaches 3.65 volts while the minimum value is 20.82% lower than the maximum value with only 2.89 volts while the Tx LED working with 400 mA forward-biased current. This figure also shows that the fluctuation increases with the increase in the forward current through Tx LED. There are three possible sources of noise and errors causing the fluctuation in the sensed values at the Rx: thermal noise, shot noise, and other noise.

1. *Thermal noise:* The rising temperature of both the transmitter LED and the lens can cause the fluctuation of the brightness of the emitting lights generated by the Tx LED. With the increase in the temperature of the Tx, the resistor of the RGB LED will decrease. The resistor of the experimental RGB LED after working for several minutes is almost half of its initial resistor (approximately 25 ohms). Besides, when the receiver works, the rising temperature of the electric circuit can introduce thermal noise which can result in the current fluctuation. To decrease the noise caused by the fluctuated temperature, we keep the system working for two minutes as a “warm start” before we start the experiments.
2. *Shot noise:* Most VLC systems are working in a high ambient light level environment, so the shot noise is the fluctuation in the electric current because of the optical power received on the Rx photo-electric surface which is consisted of the desired signals and the ambient lights in the environment. Experiments are performed to measure the influence of the ambient lights in our system by comparing the sensed voltage values at

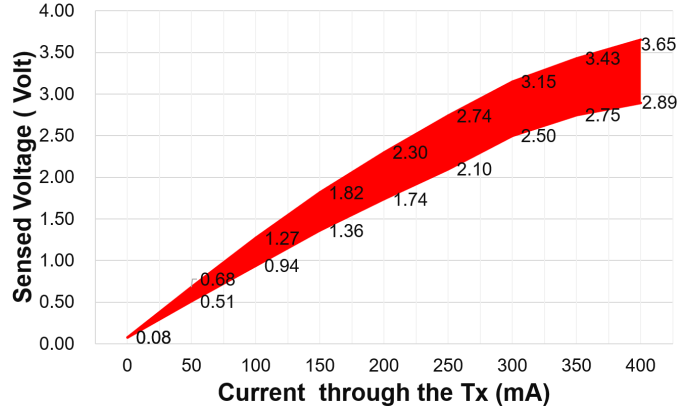


Figure 5.2: A noise example: the fluctuation of sensed voltages under Red-Red combination (Tx: Red LED; Rx: Red LED)

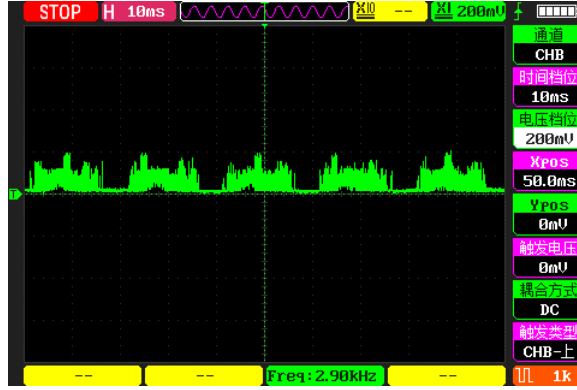


Figure 5.3: Unknown periodical noise

the Rx side in the darkroom and normal ambient light environment, and the results indicate the shot noise in our system can be neglected.

3. *Unknown noise*: During the experiments, we detect the unknown periodic noise as shown in Figure 5.3, which has a peak voltage of more than 100 mV and a frequency of 50. The change in the temperature and the incident optical power received at the Rx has no effects on the detected noise. We infer it might be caused by the hardware components in the Rx circuit and it is amplified by the TIA circuit.

### 5.3 Communication Performance

The communication accuracy of a transmitted frame  $A_{com}$  is defined in our I-VLCS system as the number of the correct bits in the frame divided by the number of total bits of the transmitted frame as shown in Equation (5.1) to indicate the performance of communication by calculating the error rate of the

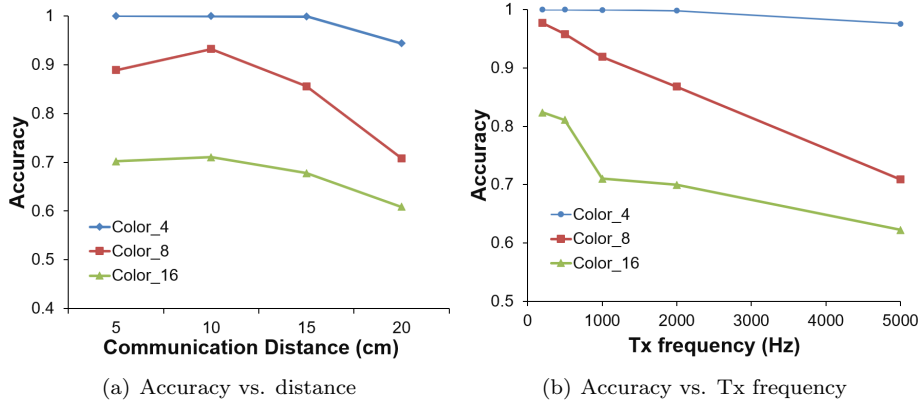


Figure 5.4: **An overview of the effects of communication distance and Tx frequencies on the communication accuracy from the tested Rx specially designed for 10 cm communication distance**

received frame.

$$A_{com} = \frac{\text{Correct bits in the frame}}{\text{Total bits of transmitted frame}} \cdot \quad (5.1)$$

The communication distance between the Tx and the Rx is an important factor affecting communication accuracy. Because the MCU of the Rx can only read a maximum 3.3-volt input at pins, the gain of the TIA circuit needs to be adjusted to obtain a good communication quality for each communication distance. The digital values converted from the sensed voltages by the inbuilt ADC of the Arduino are mapped from 0 to 1023. A too high gain in the TIA circuit will make the voltages sensed for the Tx-Rx color combinations with great responsivity such as BlueTx - BlueRx by the MCU overflowed, which will print 1023 still. While the low gain of the amplifier means that the difference of the sensed values is small, which leads to relatively low communication accuracy and increases the possibility of classifying the incoming signals into the incorrect ColorType.

The experimental results of the test Rx specific for 10 cm communication distance are shown in Figure 5.5. Except for the distance between Tx and the Rx, the transmitted frequency and the ColorMode of the frame both have a significant influence on the accuracy. The tested Tx sends the frame with five different frequencies, 200 Hz, 500 Hz, 1 kHz, 2 kHz, and 5 kHz. The maximum transmitting frequency measured for the system is 5 kHz because the Rx needs to have multiple times higher receiving frequencies compared with the transmitting frequency to guarantee communication accuracy and the chosen Rx RGB LED can not support a very high frequency when working as a photo-detector. The measured Rx is targeting the 10 cm communicate distance, and the distance measured for the experiments is up to a half meter. During the experiments, the Tx sent the frames with data generated randomly in the payload segment 10000 times for every tested distance, ModeType and transmitting frequency which will be decoded and demodulated by the Rx and send back to the PC terminal to calculate the communication accuracy.

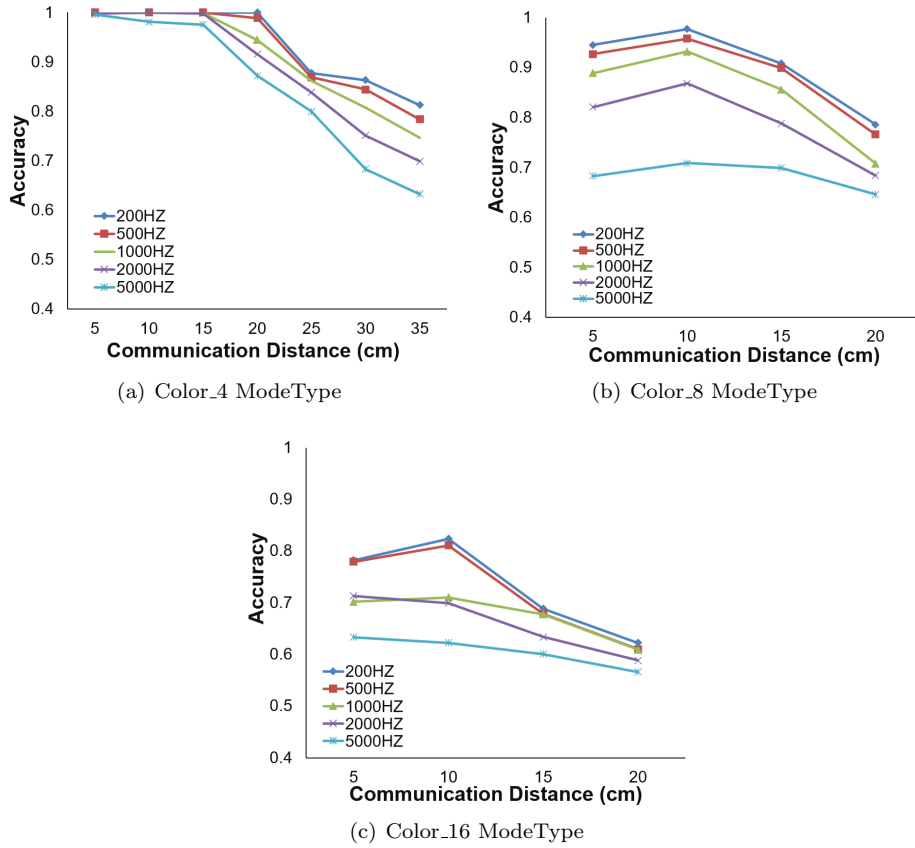


Figure 5.5: Experimental results of the average accuracy with the increase of the communication distance at different transmitting frequencies for each ModeType frame from the tested Rx specially designed for 10 cm communication distance

Figure 5.5(a) presents the results of Color\_4 ModeType frames in which each color representing 2 bits following the coding scheme in Table 3.2. The system can achieve an accuracy higher 99.99% with the transmitting frequency lower than 1 kHz and reach a 99.952% accuracy of 2 kHz frequency at 10 cm communication distance. While the accuracy decreases to 98.126% with the conditions of 5 kHz frequency and 10 cm communication distance. The Rx should achieve the maximum  $A_{com}$  at 10 cm distance based on the design of the tested Rx, and the actual results are all following the design except the data working at 5 kHz frequency which reaches a 99.633% at 5 cm higher than the 98.126% at the designed 10 cm distance. A possible reason is that the 4 ColorTypes selected in Color\_4 are easy to classify and a closer distance resulting in the higher sensed voltages at the Rx, even the sensed values are overflowed than the maximum mapping value of the ADC in the MCU but it does not affect the color recognition process at all. For example, the red sub-LED will receive a sequence of 1023 for color1Tx at 5 cm, the actually detected voltage should print a value higher than 1023 instead but it can not. And the blue and red sub-LEDs re-

ceive low values for the color1Tx. Due to the other three ColorType used for Color\_4 Mode does not meet or even close to these conditions at all, that is there is a quite big Euclidean distance calculated by the software between the values of the measured signal and the clusters of the other three ColorType. So the incoming signals will still be recognized as the color1Tx and the result of the color recognition is correct. The other three ColorTypes have similar cases while the bigger sensed values result in the higher  $A_{com}$  at 5 cm compared with 10 cm communication distance.

With the increase of communication distance, the  $A_{com}$  of Color\_4 frames decreases rapidly after 15 cm and 20 cm communication distance for the frequency higher and lower than 1 kHz respectively. The Rx only has 81.309% and 63.294% for 200 Hz and 5 kHz Tx at 35 cm communication distance. Compared with the Color\_4 ModeType, the Color\_8 ModeType in Figure 5.5(b) and Color\_16 ModeType in Figure 5.5(c) have the similar trend but a lower  $A_{com}$ , because the increase in the difficulty of color recognition results from the smaller intervals of the sensed values between each ColorType when more ColorType are used to map the values from 0 to 1023. The  $A_{com}$  of Color\_8 ModeType can achieve 99.089% at the designed communication distance while the Color\_16 ModeType can only have 82.334% accuracy. The tested performances for these two ModeTypes, especially Color\_16 ModeType are not good enough. The main reasons are the noises will be introduced in Section 5.2 and possible work can be done in Chapter 6 to further improve the accuracy.

## 5.4 Positioning Performance

Based on the experimental results from Section 3.4, we know the responsivity of each Tx - Rx combination and the green sub-LED has a low responsivity to all incoming lights which are not suitable for working as a photo-detector.

Three Tx - Rx combinations that have a great responsivity are chosen for positioning as indicated in Figure 5.6. The solid lines are the selected combinations: RedTx-RedRx, BlueTx-GreenRx, and BlueTx-BlueRx. The dotted lines are their fitting curves in high-order polynomial. The angles lower than

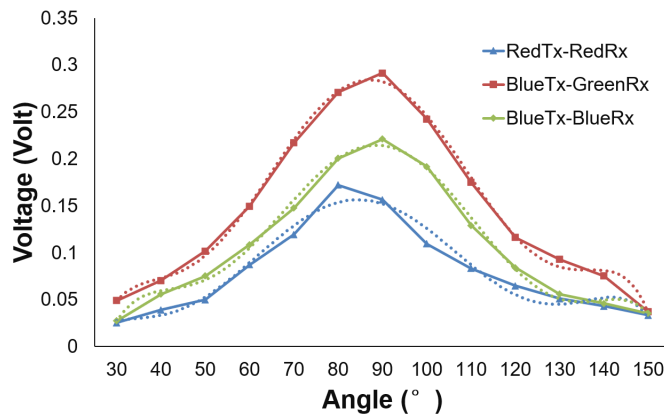


Figure 5.6: Selected Tx - Rx color combination for positioning

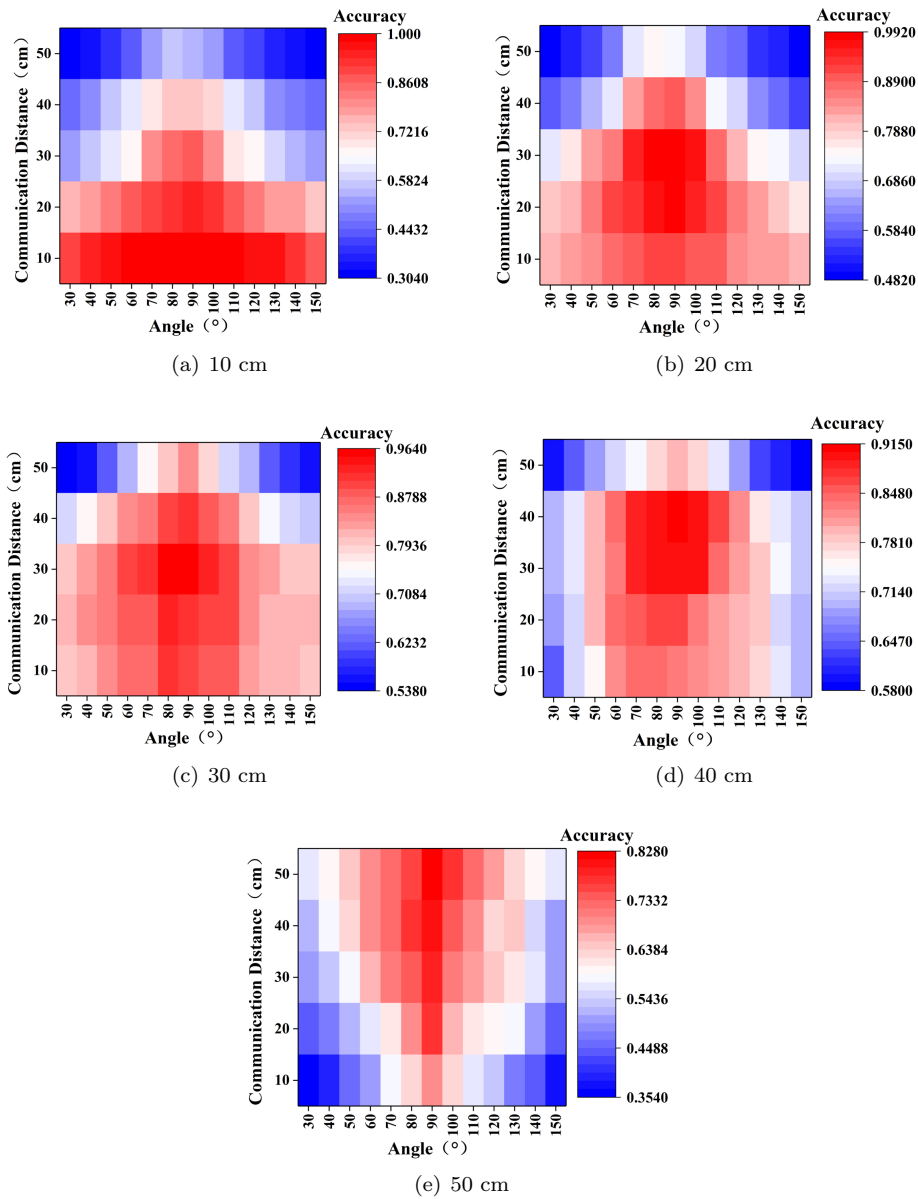


Figure 5.7: Experimental results of the positioning at each measured grid estimated by formulas calibrated at different distances from 10 cm to 50 cm at  $90^\circ$

$30^\circ$  or higher than  $150^\circ$  are not included because the sensed voltages values are very close to the read values with the ambient light only. It is obvious that the angles achieving the maximum sensed voltages reading by the Rx are  $80^\circ$ ,  $90^\circ$  and  $90^\circ$  for RedTx-RedRx, BlueTx-GreenRx and BlueTx-BlueRx Tx - Rx combination, respectively. Based on the relationship between the distance and the sensed voltages inferred in Section 3.3.2 and the fitting curves in polynomial

configured for the tested Rx, the Rx can estimate the relative location of the Tx in the Rx's coordinate during communication.

$$A_{pos} = \frac{\text{Number of correct estimation}}{\text{Total number of estimation times}} . \quad (5.2)$$

Figure 5.7 presents the positioning accuracy measured at each test grid with the different estimating formulas generated by the calibration data collected at concentric semicircles at different distances. For example, Figure 5.7(a) is the  $A_{pos}$  measured using the fitting curve and formula calibrated at the 10 cm distance. During the experiments, the Tx is located at every grid and sends Data frames with data generated randomly in the payload using Color 4 ModeType and 100 Hz frequency. The actual number of test grids is 65 (13 different degrees and 5 various distances).

The results generally follow our expects, the  $A_{pos}$  would be higher if the test grids at the online positioning process are the grids used to generate the formulas in the offline collection stage. For example, in Figure 5.7(b), the  $A_{pos}$  achieved the maximum values 99.1% at 20 cm communication distance and 80° which is the distance deployed for generating the estimating formula. While it can only achieve a maximum of 74.1% among grids at the 50 cm distance. Besides, the longer the distance from the grid to the Rx and the bigger the angle difference between the grid and 90°, the lower positioning accuracy can be achieved.

Among all estimating formulas calibrated at five different distances, the formula generated by 30 cm calibration as shown in Figure 5.7(c) has the best performance, which has a quite high  $A_{pos}$  measured at the 10 cm, 20 cm and 30 cm communication distance within the angles from 40° to 120°. It achieves a maximum 96.3%  $A_{pos}$  at 30 cm communication distance and 90°. The worst  $A_{pos}$  53.8% is got at the grid located at the right corner of the figure (50 cm, 30°). And there are 51 of 65 test grids with an accuracy higher than 80% which covers most of the measurement area.

## Chapter 6

# Conclusions and Future Work

The design of an integrated sensing and communication VLC system is a novel topic that has a lot to be exploited. The thesis proposed the I-VLCS system that leverages the advantage of LED-to-LED communication to use the existing RGB LED on the MCU to provision massive IoT devices. Its key composition includes i) the implementation of uplink and downlink LED-to-LED communication using RGB LEDs between the Tx and the RX; ii) The proposed positioning algorithms to estimate the Tx relative relation in two-dimensional based on the Rx's frame using only one pair of RGB LEDs. The I-VLCS system has been implemented with the off-the-shelf high-power RGB LEDs, low-cost electronic components, and cost-efficient MCU Arduino Due. Experimental results have demonstrated that the system can achieve a communication accuracy higher than 99.999% at the designed communication distance using the Color\_4 Mode and have a good performance in positioning as well. I believe that more researches could be done to explore the possibility of the RGB LED-to-LED communication which provides high data rates and widely applied scenarios. The implementation of integrated sensing and communication in VLC is an interesting topic to solve many indoor location challenges as well.

The proof-of-concept of the I-VLCS system has been designed, developed, evaluated and presented in the project. There are still lots of possible future work that can be done to extend the functionality and improve the performance of the system: i) Although the Color\_4 Mode achieves high accuracy in both communication and positioning, the Color\_8 Mode has only an acceptable communication accuracy and the designed Color\_16 Mode is not good enough to perform the communication. To implement this, there are two directions: the software and the hardware. The hardware design of our system is not professional enough which leads to the unknown noise presented in Section 5.2. Although both Tx and Rx circuit is designed with a PCB, there are still some circuits that are built on breadboard. In the perspective of the software, the classification algorithm implemented in the color recognition process is the k-NN which is simple but needs lots of data for training. Other algorithms like the Naive Bayesian Classifier (NBC) is tried during our project but was not taken because it gives worse feedback in the accuracy. We believe a good clas-

sification algorithm like Artificial Neural Network (ANN) can achieve a higher communication accuracy. ii) The proposed positioning algorithm is based on the RSS model and uses the characteristics that the R, G, B sub-LEDs have different responsivity to the incoming signals with different wavelengths and it only works for two dimensional. Other positioning models such as AOA can be further researched to implement a three-dimensional positioning algorithm using only one RGB LED. iii) The communication distance needs to be extended to at least several meters for provisioning massive IoT devices. However, it is limited by the power of the LEDs which is the 3W RGB LED implemented in the designed I-VLCS system to simulate the existing RGB LED on IoT devices.

# Appendix A

## A.1: The states of Tx

State	Condition	Description
INIT	Power on the MCU or received the <b>INIT_ACK</b>	The initial state of the Tx, the system keeps waiting the command from the PC terminal.
EST	Received the <b>CHAN_ACK</b> when the system is at <b>WAIT</b> state.	The communication channel between the Tx and the Rx is established.
CAL	Received the <b>CAL_ACK</b> when the system is at <b>WAIT</b> state.	The calibration process is done.
COM	Received the <b>COM_ACK</b> when the system is at <b>WAIT</b> state.	The Tx system is in the communication state.
WAIT	After the Tx received the command from the PC terminal and sent any Request signal to the Rx, the state of the Tx will transform into <b>WAIT</b> state.	The Tx system is waiting for any Acknowledge signal from the Rx.

## A.2 The states of Rx

<b>State</b>	<b>Condition</b>	<b>Description</b>
INIT	Power on the MCU or received the <b>INIT_REQ</b> or <b>INIT_CMD</b>	The initial state of the Rx, the system keeps waiting the Request signal from the Tx
EST	Received the <b>CHAN_REQ</b>	The system will send <b>CHAN_ACK</b> signal and transform into <b>EST</b> state.
CAL	Received the <b>CAL_REQ</b>	The system will send <b>CAL_ACK</b> signal and transform into CAL state.
COM	Received the <b>COM_REQ</b> or <b>COM_CMD</b>	The system will send <b>COM_ACK</b> signal and transform into <b>COM</b> state.
POS	Received the <b>POS_CMD</b>	The system will transform into <b>POS</b> state.

# Bibliography

- [1] Arduino due. <https://store-usa.arduino.cc/products/arduino-due>.
- [2] Wi-fi halow: Low power, long-range wi-fi® for iot, 2020. <https://www.wi-fi.org/discover-wi-fi/wi-fi-certified-halow>.
- [3] Wi-fi halow: Wi-fi for iot applications” by wi-fi alliance, may 2020.
- [4] Ieee standard for information technology–telecommunications and information exchange between systems - local and metropolitan area networks–specific requirements - part 11: Wireless lan medium access control (mac) and physical layer (phy) specifications amendment 2: Sub 1 ghz license exempt operation. *IEEE Std 802.11ah-2016 (Amendment to IEEE Std 802.11-2016, as amended by IEEE Std 802.11ai-2016)*, pages 1–594, 2017.
- [5] G Corbellini, K. Aksit, S. Schmid, S. Mangold, and T. R Gross. Connecting networks of toys and smartphones with visible light communication. *IEEE Communications Magazine*, 52(7):72–78, 2014.
- [6] P. H. Dietz, W. S. Yerazunis, and D Leigh. Very low-cost sensing and communication using bidirectional leds. In *UbiComp 2003: Ubiquitous Computing, 5th International Conference, Seattle, WA, USA, October 12-15, 2003, Proceedings*, 2003.
- [7] S. Dimitrov and H. Haas. *Principles of LED Light Communications: Towards Networked Li-Fi*. Principles of LED Light Communications: Towards Networked Li-Fi, 2015.
- [8] Trong-Hop Do, Junho Hwang, and Myungsik Yoo. Tdoa based indoor visible light positioning systems. In *2013 Fifth International Conference on Ubiquitous and Future Networks (ICUFN)*, pages 456–458, 2013.
- [9] Y. Feng, Y. Zhao, and F. Gunnarsson. Proximity report triggering threshold optimization for network-based indoor positioning. In *International Conference on Information Fusion*, 2015.
- [10] M. Galal, W. P. Ng, R. Binns, and Aae Aziz. Characterization of rgb leds as emitter and photodetector for led-to-led communication. In *2020 12th International Symposium on Communication Systems, Networks and Digital Signal Processing (CSNDSP)*, 2020.
- [11] Mariam Galal, Wai Pang Ng, Richard Binns, and Ahmed Abd El Aziz. Experimental characterization of rgb led transceiver in low-complexity led-to-led link. *Sensors*, 20(20), 2020.

- [12] Mariam Galal, Wai Pang Ng, Richard Binns, and Ahmed Abd El Aziz. Characterization of rgb leds as emitter and photodetector for led-to-led communication. In *2020 12th International Symposium on Communication Systems, Networks and Digital Signal Processing (CSNDSP)*, pages 1–6, 2020.
- [13] Domenico Giustiniano, Nils Ole Tippenhauer, and Stefan Mangold. Low-complexity visible light networking with led-to-led communication. In *2012 IFIP Wireless Days*, pages 1–8, 2012.
- [14] L. Grobe, A. Paraskevopoulos, J. Hilt, and D. Schulz. High-speed visible light communication systems. *IEEE Communications Magazine*, 51(12):60–66, 2013.
- [15] W. Gu, W. Zhang, M. Kavehrad, and L. Feng. Three-dimensional light positioning algorithm with filtering techniques for indoor environments. *Optical Engineering*, 53(10):107107.1–107107.11, 2014.
- [16] H. Haas. Lifi: Conceptions, misconceptions and opportunities. In *2016 IEEE Photonics Conference (IPC)*, 2016.
- [17] H. Haas and C. Cheng. What is lifi? In *2015 European Conference on Optical Communication (ECOC)*, 2015.
- [18] S. W. Ho, Y. Muhammad, and Badri Narayanan Vellambi Ravisankar. Visible light based indoor positioning system. 2017.
- [19] S. Y. Jung, S. Hann, and C. S. Park. Tdoa-based optical wireless indoor localization using led ceiling lamps. *IEEE Transactions on Consumer Electronics*, 57(4):1592–1597, 2012.
- [20] J. M Kahn and J. R Barry. Wireless infrared communications. *Proceedings of the IEEE*, 85(2):265–298, 2002.
- [21] D Karunatilaka, F. Zafar, V. Kalavally, and R. Parthiban. Led based indoor visible light communications: State of the art. *IEEE Communications Surveys Tutorials*, 17(3):1649–1678, 2015.
- [22] M. Kowalczyk and J. Siuzdak. Vlc link with leds used as both transmitters and photo-detectors. *IEEE*, 2015.
- [23] Liqun Li, Pan Hu, Chunyi Peng, Jacky Shen, Zhao, and Feng. Epsilon: A visible light based positioning system. *USENIX Association*, 2014.
- [24] S. Li, B. Huang, and Z. Xu. [ieee 2017 ieee globecom workshops (gc wkshps) - singapore, singapore (2017.12.4-2017.12.8)] 2017 ieee globecom workshops (gc wkshps) - experimental mimo vlc systems using tricolor led transmitters and receivers. 2017.
- [25] P. Lou, H. Zhang, Z. Xie, M. Yao, and Z. Xu. Fundamental analysis for indoor visible light positioning system. In *2012 1st IEEE International Conference on Communications in China Workshops (ICCC)*, 2012.
- [26] M., Kowalczyk, J., and Siuzdak. Photo-reception properties of common leds. *Opto-Electronics Review*, 25(3):222–228, 2017.

- [27] Muhammad Sarmad Mir, Behnaz Majleseini, Borja Genovés Guzmán, Julio Torres, and Domenico Giustiniano. Led-to-led based vlc systems: developments and open problems. pages 1–6, 06 2021.
- [28] E. Miyazaki, S. Itami, and T. Araki. Using a light-emitting diode as a high-speed, wavelength selective photodetector. *Review of Scientific Instruments*, 69(11):3751–3754, 1998.
- [29] U. Nadeem, N Hassan, M Pasha, and C. Yuen. Indoor positioning system designs using visible led lights: performance comparison of tdm and fdm protocols. *Electronics Letters*, 51(1):72–74, 2014.
- [30] H. Park and J. R. Barry. Trellis-coded multiple-pulse position modulation for wireless infrared communications. In *IEEE Global Telecommunications Conference*, 1998.
- [31] P. H. Pathak, X. Feng, P. Hu, and P. Mohapatra. Visible light communication, networking, and sensing: A survey, potential and challenges. *IEEE Communications Surveys Tutorials*, 17(4):2047–2077, 2015.
- [32] R. S. Romaniuk, M. Kowalczyk, and J. Siuzdak. Influence of reverse bias on the leds properties used as photo-detectors in vlc systems. In *XXXVI Symposium on Photonics Applications in Astronomy*, page 966205, 2015.
- [33] K. Sato, T. Ohtsuki, I. Sasase, and S. Mori. Performance analysis of (m, 2) mppm with imperfect slot synchronization. In *IEEE Pacific Rim Conference on Communications, Computers Signal Processing*, 1993.
- [34] S. Schmid, G. Corbellini, S. Mangold, and T. R. Gross. An led-to-led visible light communication system with software-based synchronization. In *Globecom Workshops (GC Wkshps), 2012 IEEE*, 2012.
- [35] S. Schmid, G. Corbellini, S. Mangold, and T. R. Gross. Continuous synchronization for led-to-led visible light communication networks. In *International Workshop in Optical Wireless Communications*, 2014.
- [36] Stefan Schmid, Giorgio Corbellini, Stefan Mangold, and Thomas R. Gross. Led-to-led visible light communication networks. In *Fourteenth Acm International Symposium on Mobile Ad Hoc Networking Computing*, page 1, 2013.
- [37] A. Sevincer, A. Bhattarai, M. Bilgi, M. Yuksel, and N. Pala. Lightnets: Smart lighting and mobile optical wireless networks - a survey. *IEEE Communications Surveys Tutorials*, 15(4):1620–1641, 2013.
- [38] G. Stepniak, M. Kowalczyk, L. Maksymiuk, and J. Siuzdak. Transmission beyond 100 mbit/s using led both as a transmitter and receiver. *IEEE Photonics Technology Letters*, 27(19):2067–2070, 2015.
- [39] Jayakorn Vongkulbhisal, Bhume Chantaramolee, Yan Zhao, and Waleed S. Mohammed. A fingerprinting-based indoor localization system using intensity modulation of light emitting diodes. *Microwave Optical Technology Letters*, 54(5):1218–1227, 2012.

- [40] Wang, Y., Chi, and N. Demonstration of high-speed  $2 \times 2$  non-imaging mimo nyquist single carrier visible light communication with frequency domain equalization. *Lightwave Technology*, 2014.
- [41] L. C. Wu and H. M. Tsai. Modeling vehicle-to-vehicle visible light communication link duration with empirical data. In *Globecom Workshops*, 2013.
- [42] Yang, Se-Hoon, Jung, Eun-Mi, Han, and Sang-Kook. Indoor location estimation based on led visible light communication using multiple optical receivers. *Communications Letters, IEEE*, 2013.
- [43] S. H. Yang, E. M. Jeong, D. R. Kim, H. S. Kim, Y. H. Son, and S. K. Han. Indoor three-dimensional location estimation based on led visible light communication. *Electronics Letters*, 49(1):54–55, 2013.
- [44] Shun Hsiang You, Shih Hao Chang, Hao Min Lin, and Hsin Mu Tsai. Visible light communications for scooter safety. In *Proceeding of the 11th annual international conference on Mobile systems, applications, and services*, 2013.
- [45] S. H. Yu, O. Shih, H. M. Tsai, and R. D. Roberts. Smart automotive lighting for vehicle safety. *IEEE Communications Magazine*, 51(12):50–59, 2013.
- [46] Y. Zhao, F. Yin, F. Gunnarsson, M. Amirijoo, Emre Özkan, and F. Gustafsson. Particle filtering for positioning based on proximity reports. *IEEE*, 2015.
- [47] Y. Zhuang, L. Hua, L. Qi, J. Yang, P. Cao, Y. Cao, Y. Wu, J. Thompson, and H. Haas. A survey of positioning systems using visible led lights. *IEEE Communications Surveys Tutorials*, pages 1–1, 2018.